Topological phase transition on the edge of two-dimensional $\mathbb{Z}_2$ topological order

Wei-Qiang Chen,[1,2,3,*] Chao-Ming Jian,[4,†] Liang Kong,[2,5,7,‡] Yi-Zhuang You,[6,§] and Hao Zheng[2,5,7,8,‖]

[1]*Department of Physics, Southern University of Science and Technology, Shenzhen 518055, China*
[2]*Shenzhen Institute for Quantum Science and Engineering, Southern University of Science and Technology, Shenzhen 518055, China*
[3]*Shenzhen Key Laboratory of Advanced Quantum Functional Materials and Devices, Southern University of Science and Technology, Shenzhen 518055, China*
[4]*Kavli Institute for Theoretical Physics, University of California Santa Barbara, California 93106, USA*
[5]*Guangdong Provincial Key Laboratory of Quantum Science and Engineering, Southern University of Science and Technology, Shenzhen 518055, China*
[6]*Department of Physics, University of California, San Diego, California 92093, USA*
[7]*Shenzhen Key Laboratory of Quantum Science and Engineering, Southern University of Science and Technology, Shenzhen,518055, China*
[8]*Department of Mathematics, Peking University, Beijing 100871, China*

(Received 10 April 2020; revised 22 June 2020; accepted 23 June 2020; published 23 July 2020)

The unified mathematical theory of gapped and gapless edges of two-dimensional (2d) topological orders was developed by two of the authors. According to this theory, the critical point of a purely edge topological phase transition of a 2d topological order can be mathematically characterized by an enriched fusion category. In this work, we provide a physical proof of this fact in a concrete example: the 2d $\mathbb{Z}_2$ topological order. In particular, we construct an enriched fusion category, which describes a gappable nonchiral gapless edge of the 2d $\mathbb{Z}_2$ topological order. Then, we use an explicit lattice model construction to realize a topological phase transition between the two well-known gapped edges of the 2d $\mathbb{Z}_2$ topological order, and show that all the ingredients of the above enriched fusion category can be realized explicitly in this lattice model.

DOI: 10.1103/PhysRevB.102.045139

I. INTRODUCTION

The subject of topological order has attracted a lot of attention in recent years among physicists. The main reason is that topological orders are new phases of matter that go beyond Landau's paradigm of phases and phase transitions (see a recent review [1] and references therein). Landau's paradigm is based on a symmetry-broken theory. The mathematical theory of symmetry is that of groups. The new phases of matter challenge us to find radically new mathematical language and tools to understand topological phases and phase transitions. In this work, we show that the critical point of a purely edge topological phase transition between two gapped edges of the same two-dimensional (2d) topological order can be precisely described by a mathematical structure called an enriched fusion category [2,3]. Throughout this work, we use "nd" to represent the spatial dimension and "$(n+1)$D" to represent the space-time dimension.

A gapped edge of a 2d anomaly-free topological order can be viewed as an anomalous one-dimensional (1d) topological order. It contains no local observables (such as correlation functions) in the long-wavelength limit except topological excitations, which can be fused among themselves and form a unitary fusion category (UFC) [4,5]. A topological phase transition restricted on the 1d edge (without altering the 2d bulk) will be called a purely edge topological phase transition (see, for example, [6]). Observe that the gap in a neighborhood of the edge must be closed at the critical point. Therefore, *the critical point of a purely edge topological phase transition should be nothing but a gappable nonchiral gapless edge of a 2d anomaly-free topological order.* As a consequence, to ask for a precise mathematical description of the critical points of purely edge topological phase transitions is equivalent to ask for that of the gappable nonchiral gapless edges of 2d anomaly-free topological orders.

Based on a mixture of physical intuition and mathematical arguments, two of the authors established in [7,8] a unified mathematical theory of both gapped and gapless edges of 2d anomaly-free topological orders. This theory allows us to treat gapped, chiral gapless, and (gappable) nonchiral gapless edges on an equal footing. More precisely, it says that all physical observables on a gapped/gapless edge form an enriched fusion category, whose Drinfeld center is precisely the unitary modular tensor category (UMTC) of the 2d bulk. Therefore, the critical point of a purely edge topological phase transition, or a gappable nonchiral gapless edge, is precisely described by an enriched fusion category. The complete mathematical theory of (gappable) nonchiral gapless edges is given in [8].

The main goal of this work is to provide a physical and lattice-model realization of all ingredients of the enriched fusion category associated to the critical point of the purely edge phase transition between the two gapped edges of the

*chenwq@sustech.edu.cn
†cmjian@kitp.ucsb.edu
‡kongl@sustech.edu.cn
§yzyou@ucsd.edu
‖hzheng@math.pku.edu.cn

2d $\mathbb{Z}_2$ topological order [9,10]. Possible experimental realizations of the two types of gapped edges are discussed in [11]. Therefore, an understanding of the topological transition between them has both theoretical and experimental interest. The main result of this work is summarized below.

(1) In Sec. III C, we give an explicit construction of a gappable nonchiral gapless edge of the 2d $\mathbb{Z}_2$ topological order given by the following triple:

$$(V \otimes_{\mathbb{C}} \overline{V},\ \mathbf{Ising} \boxtimes \overline{\mathbf{Ising}},\ (\mathbf{Ising} \boxtimes \overline{\mathbf{Ising}})_A). \tag{1}$$

(a) V is the Ising chiral algebra or vertex operator algebra (VOA) of central charge $\frac{1}{2}$ and $\overline{V}$ is the same VOA but contains only antichiral fields $\phi(\bar{z})$, $\forall\ \phi \in V$, and $V \otimes \overline{V}$ is called a nonchiral symmetry [8].

(b) **Ising** is the UMTC of V-modules, i.e., $\mathbf{Ising} = \mathrm{Mod}_V$. It contains three simple objects $\mathbf{1}, \psi, \sigma$ (with the fusion rule $\sigma \otimes \sigma = \mathbf{1} \oplus \psi$); $\overline{\mathbf{Ising}}$ is the same tensor category as **Ising** but with the braidings defined by the antibraidings in **Ising**.

(c) $\mathbf{Ising} \boxtimes \overline{\mathbf{Ising}}$ is nothing but the Drinfeld center of **Ising**, i.e.,

$$Z(\mathbf{Ising}) = \mathbf{Ising} \boxtimes \overline{\mathbf{Ising}}.$$

(d) $A = \mathbf{1} \boxtimes \mathbf{1} \oplus \psi \boxtimes \psi$ is a condensable algebra in $Z(\mathbf{Ising})$ (see Definition 3), and $Z(\mathbf{Ising})_A$ denotes the category of right A-modules in $Z(\mathbf{Ising})$ (see Definition 2). Moreover, $Z(\mathbf{Ising})_A$ is a UFC.

The enriched fusion category is determined by the pair $(Z(\mathbf{Ising}),\ Z(\mathbf{Ising})_A)$ via the standard construction [2]. More precisely,

(a) the objects in the enriched fusion category are the same as those in $Z(\mathbf{Ising})_A$;

(b) the space of morphism $\hom(x, y)$ is defined by the internal hom $[x, y] = (y \otimes_A x^*)^*$ in $Z(\mathbf{Ising})$; the internal hom $[x, y]$ can be interpreted either as the domain wall between two boundary CFTs with boundary conditions x and y, respectively, or as the partition function of a CFT defined on a strip with two boundary conditions x and y (see Fig. 4).

(2) In Sec. III E, we recall another construction of a slightly different gappable gapless edge [8]. This edge has a slightly larger nonchiral symmetry given by A, and all the rest ingredients are already included in the edge [Eq. (1)].

(3) In Sec. IV, we construct a lattice model to realize the critical point of the purely edge phase transition between two gapped edges of the $\mathbb{Z}_2$ topological order and, at the same time, all ingredients $[x, y]$ of the enriched fusion category in [Eq. (1)].

The significance of this work is twofold: (1) it provides the first lattice model realization of all ingredients of the enriched fusion category; (2) it shows that the theory developed in [7,8] can indeed provide a mathematical theory of all purely edge topological phase transitions. Since the (enriched) categorical language is not so familiar to condensed matter physicists and the lattice model construction might not be so familiar to mathematical physicists, in order to invite readers from both communities, we have tried to be self-contained.

Remark 1. We would like to remark on how to read this paper. Since our main goal is to provide a lattice model realization of ingredients of the enriched fusion category used in the mathematical theory of gapless edges of 2d topological orders, it is reasonable to explain the mathematical theory and enriched fusion category first (in Secs. II and III) and discuss the lattice model realization later (in Sec. IV). For physically oriented readers, if you encounter difficulties in Secs. II and III, we recommend you to read Sec. IV first and return to Secs. II and III later. Section IV is completely written in the usual language in physics.

II. CATEGORICAL PRELIMINARIES

In this section, we review some basic ingredients of a unitary modular tensor category (UMTC), and give two examples, and set our notations along the way.

A. Unitary modular tensor categories

It is well known that an anomaly-free 2d topological order without symmetry is described by a pair $(\mathcal{C}, c)$, where $\mathcal{C}$ is a UMTC of topological excitations (or anyons in this case) and c is the chiral central charge [12]. The category of topological excitations is not enough to fully characterize a topological order because there are nontrivial invertible topological orders that have no topological excitations. A 2d invertible topological order is given by a tensor product of the E_8 states. The chiral central charge of the E_8 state is 8. Therefore, a 2d invertible topological order can be uniquely determined by its chiral central charge, and an anomaly-free 2d topological order can be determined by a pair $(\mathcal{C}, c)$.

We review some important ingredients of a UMTC $\mathcal{C}$. It has finitely many simple objects (simple anyons). We denoted the simple objects by $i, j, k \in \mathrm{Irr}(\mathcal{C})$, where $\mathrm{Irr}(\mathcal{C})$ is the finite set of the equivalence classes of simple objects. A generic object in $\mathcal{C}$ is a direct sum of simple ones, e.g., $i \oplus j \oplus k$, and is called a composite anyon. For each pair (x, y) of objects, the hom space $\hom_{\mathcal{C}}(x, y)$ is a finite-dimensional Hilbert space. It has a tensor product functor $\otimes : \mathcal{C} \times \mathcal{C} \to \mathcal{C}$, i.e., $(x, y) \mapsto x \otimes y$, $\forall\ x, y \in \mathcal{C}$, such that it is associative, i.e., there exists an isomorphism $x \otimes (y \otimes z) \xrightarrow{\alpha_{x,y,z}} (x \otimes y) \otimes z$ for all $x, y, z \in \mathcal{C}$ satisfying necessary coherence conditions (i.e., pentagon relation). These data can be reduced to the induced linear isomorphisms $\hom_{\mathcal{C}}(i \otimes (j \otimes k), l) \simeq \hom_{\mathcal{C}}((i \otimes j) \otimes k, l)$ for $i, j, k, l \in \mathrm{Irr}(\mathcal{C})$ or, equivalently, to F matrices, which satisfies pentagon identities. The dimension of $\hom(i \otimes j, k)$, denoted by N_{ij}^k, is called the fusion rule. The category $\mathcal{C}$ has a tensor unit $\mathbf{1}$, which is simple, together with unit isomorphisms $\mathbf{1} \otimes x \xrightarrow{l_x} x \xleftarrow{r_x} x \otimes \mathbf{1}$ for all $x \in \mathcal{C}$ satisfying necessary coherence conditions (i.e., triangle relation). It has a unitary structure. More precisely, for each morphism $f : x \to y$, there is an adjoint morphism $f^\dagger : y \to x$ such that

$$(g \otimes h)^\dagger = g^\dagger \otimes h^\dagger, \qquad \forall\ g : v \to w, h : x \to y, \tag{2}$$

$$\alpha_{x,y,z}^\dagger = \alpha_{x,y,z}^{-1}, \quad l_x^\dagger = l_x^{-1}, \quad r_x^\dagger = r_x^{-1}. \tag{3}$$

For each $x \in \mathcal{C}$, there is a dual object x^* (the antiparticle of x), together with the duality morphisms (the creation and

annihilation operators) expressed graphically as follows:

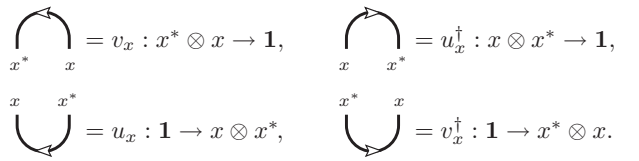

(4)

which satisfy necessary coherence properties. The quantum dimension of an object x is defined by $\dim x = v_x \circ v_x^\dagger = u_x^\dagger \circ u_x$, both of which are elements of $\hom_{\mathcal{C}}(\mathbf{1}, \mathbf{1}) = \mathbb{C}$. The quantum dimension of the category is defined by $\dim \mathcal{C} := \sum_{i \in \mathrm{Irr}(\mathcal{C})} (\dim i)^2$. It is known that $\dim x > 0$ for $x \in \mathcal{C}$ [13, Theorem 2.3; Corollary 2.10]. In particular, $\dim \mathcal{C} \geqslant 1$. We denote the positive square root of $\dim \mathcal{C}$ by $\sqrt{\dim \mathcal{C}}$.

It has a braiding structure, which amounts to an isomorphism $x \otimes y \xrightarrow{b_{x,y}} y \otimes x$ for all $x, y \in \mathcal{C}$ satisfying necessary coherence conditions (i.e., hexagon relations), and we have $b_{x,y}^\dagger = b_{x,y}^{-1}$. The braiding satisfies a nondegenerate condition, which says that the so-called S matrix

$$s_{i,j} = \frac{1}{\sqrt{\dim \mathcal{C}}} \qquad (5)$$

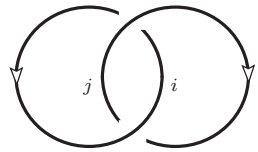

is nondegenerate. Each simple object $i \in \mathrm{Irr}(\mathcal{C})$ has a topological spin $\theta_i \in \mathbb{C}$, which is also called a twist in mathematics. In physics, the condition $\theta_i = 1$ for $i \in \mathrm{Irr}(\mathcal{C})$ amounts to say that the simple anyon i is a boson.

Let us fix an orthonormal basis $\{\lambda_{ij}^{k;\alpha}\}_{\alpha=1}^{N_{ij}^k}$ in $\hom_{\mathcal{C}}(i \otimes j, k)$ and its dual basis $\{y_{k;\beta}^{ij}\}_{\beta=1}^{N_{ij}^k}$ in $\hom_{\mathcal{C}}(k, i \otimes j)$, i.e.,

$$\begin{aligned} y_{k;\beta}^{ij} &= \left(\lambda_{ij}^{k;\beta}\right)^\dagger, \\ \lambda_{ij}^{k;\alpha} \circ y_{k;\beta}^{ij} &= \delta_{\alpha,\beta}\, \mathrm{id}_k, \\ \sum_{k,\beta} y_{k;\beta}^{ij} \circ \lambda_{ij}^{k;\beta} &= \mathrm{id}_{i\otimes j}. \end{aligned} \qquad (6)$$

We denote the basis vectors graphically as follows:

$$\lambda_{ij}^{k;\alpha} = \qquad , \qquad y_{k;\alpha}^{ij} = \qquad . \qquad (7)$$

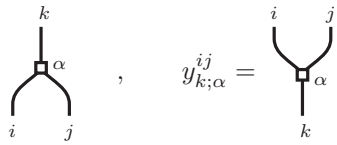

If $N_{ij}^k = 1$, we abbreviate $\lambda_{ij}^{k;1}$ by λ_{ij}^k and $y_{k;1}^{ij}$ by y_k^{ij}. We also fix

$$\lambda_{\mathbf{1}i}^i = l_i, \quad \lambda_{i\mathbf{1}}^i = r_i \quad \Rightarrow \quad y_{\mathbf{1}i}^i = l_i^{-1}, \quad y_{i\mathbf{1}}^i = r_i^{-1}. \qquad (8)$$

Remark 2. The simplest example of UMTC is the trivial one **H**, which is the category of finite-dimensional Hilbert spaces. It has a unique simple object (i.e., the tensor unit $\mathbf{1}$) given by the one-dimensional Hilbert space $\mathbb{C}$. The pair $(\mathbf{H}, 0)$ describes the trivial 2d topological order.

B. Toric code and Ising UMTC's

In this section, we give two examples of UMTC's: toric code UMTC and Ising UMTC, both of which are important to this work.

Example 1. We denote the toric code UMTC by **Toric**. We list some of its ingredients below:

(1) There are only four simple objects $\mathbf{1}, e, m, f$.

(2) The fusion rules are given by $e \otimes m = f, e \otimes e = m \otimes m = f \otimes f = \mathbf{1}$. This implies that $e^* = e$, $m^* = m$, $f^* = f$ and we have $\dim \mathbf{1} = \dim e = \dim m = \dim f = 1$.

(3) Topological spins: $\theta_x = 1$ for $x = \mathbf{1}, e, m$ and $\theta_f = -1$.

(4) S matrix is given by

$$S = \frac{1}{2}\begin{pmatrix} 1 & 1 & 1 & 1 \\ 1 & 1 & -1 & -1 \\ 1 & -1 & 1 & -1 \\ 1 & -1 & -1 & 1 \end{pmatrix}.$$

Remark 3. The name of **Toric** comes from the fact that the pair (**Toric**, 0) describes the $\mathbb{Z}_2$ 2d topological order, whose first lattice model realization is given by the toric code model [9]. For readers with a mathematical background, **Toric** is nothing but the Drinfeld center $Z(\mathcal{R}\mathrm{ep}(\mathbb{Z}_2))$ of the category $\mathcal{R}\mathrm{ep}(\mathbb{Z}_2)$ of finite-dimensional representations of the group $\mathbb{Z}_2$.

Example 2. We denote the Ising UMTC by **Ising**. We list some of its ingredients below:

(1) There are three simple objects $\mathbf{1}, \psi, \sigma$ all isomorphic to their duals, i.e., $\mathbf{1} = \mathbf{1}^*$, $\psi = \psi^*$, and $\sigma = \sigma^*$. Their quantum dimensions are given by $\dim \mathbf{1} = \dim \psi = 1$ and $\dim \sigma = \sqrt{2}$.

(2) The fusion rules are defined by $\psi \otimes \psi = \mathbf{1}$, $\psi \otimes \sigma = \sigma$, $\sigma \otimes \sigma = \mathbf{1} \oplus \psi$.

(3) Associators: we choose a basis such that the associators can be expressed in terms of F matrices. In addition to (8), we further require

$$\lambda_{\psi\psi}^{\mathbf{1}} = v_\psi, \quad y_{\mathbf{1}}^{\psi\psi} = u_\psi, \quad \lambda_{\sigma\sigma}^{\mathbf{1}} = \frac{1}{\sqrt{2}}\, v_\sigma, \quad y_{\mathbf{1}}^{\sigma\sigma} = u_\sigma. \qquad (9)$$

There exists a choice of remaining basis, which is unique up to an arbitrary choice of $\lambda_{\psi\sigma}^{\sigma}$ (or, equivalently, a choice of $\lambda_{\sigma\psi}^{\sigma}$ or $\lambda_{\sigma\sigma}^{\psi}$), realizing the following F matrices:

$$\begin{aligned} &(\psi \otimes \sigma) \otimes \psi = \sigma \xrightarrow{-1} \sigma = \psi \otimes (\sigma \otimes \psi), \\ &(\sigma \otimes \psi) \otimes \sigma \xrightarrow{\lambda_{\sigma\psi}^{\sigma} \otimes 1} \sigma \otimes \sigma \xrightarrow{\lambda_{\sigma\sigma}^{\mathbf{1}} \oplus \lambda_{\sigma\sigma}^{\psi}} \mathbf{1} \oplus \psi \xrightarrow{1 \oplus -1} \mathbf{1} \oplus \psi \xrightarrow{y_{\mathbf{1}}^{\sigma\sigma} \oplus y_{\psi}^{\sigma\sigma}} \sigma \otimes \sigma \xrightarrow{1 \otimes y_{\sigma}^{\psi\sigma}} \sigma \otimes (\psi \otimes \sigma), \\ &(\sigma \otimes \sigma) \otimes \sigma \xrightarrow{\cong} (\mathbf{1} \otimes \sigma) \oplus (\psi \otimes \sigma) \xrightarrow{\begin{pmatrix} \frac{1}{\sqrt{2}} & \frac{1}{\sqrt{2}} \\ \frac{1}{\sqrt{2}} & -\frac{1}{\sqrt{2}} \end{pmatrix}} (\sigma \otimes \mathbf{1}) \oplus (\sigma \otimes \psi) \xrightarrow{\cong} \sigma \otimes (\sigma \otimes \sigma), \end{aligned} \qquad (10)$$

where we have only spelled out those nontrivial ones.

(4) Braidings:

$$\mathbf{1}\otimes x = x \xrightarrow{b_{\mathbf{1},x}=1} x = x\otimes\mathbf{1} \quad \text{for } x = \mathbf{1}, \psi, \sigma;$$

$$\psi\otimes\psi = \mathbf{1} \xrightarrow{b_{\psi,\psi}=-1} \mathbf{1} = \psi\otimes\psi;$$

$$\psi\otimes\sigma = \sigma \xrightarrow{b_{\psi,\sigma}=e^{-\frac{\pi i}{2}}} \sigma = \sigma\otimes\psi;$$

$$\sigma\otimes\psi = \sigma \xrightarrow{b_{\sigma,\psi}=e^{-\frac{\pi i}{2}}} \sigma = \psi\otimes\sigma;$$

$$\sigma\otimes\sigma = \mathbf{1}\oplus\psi \xrightarrow{b_{\sigma,\sigma}=e^{-\frac{\pi i}{8}}\oplus e^{\frac{3\pi i}{8}}} \mathbf{1}\oplus\psi = \sigma\otimes\sigma. \qquad (11)$$

(5) Spins: $\theta_{\mathbf{1}} = 1, \theta_\psi = -1, \theta_\sigma = e^{\frac{\pi i}{8}}$.

(6) S matrix:

$$S = \frac{1}{2}\begin{pmatrix} 1 & 1 & \sqrt{2} \\ 1 & 1 & -\sqrt{2} \\ \sqrt{2} & -\sqrt{2} & 0 \end{pmatrix}.$$

Remark 4. The UMTC **Ising** can be realized as the category of modules over the Ising vertex operator algebra V with central charge $c = \frac{1}{2}$, i.e., **Ising** $= \mathrm{Mod}_V$. In particular, V has three irreducible V-modules with the lowest conformal weights given by $0, \frac{1}{2}, \frac{1}{16}$, corresponding to three simple objects $\mathbf{1}, \psi, \sigma$, respectively.

Remark 5. We use $\overline{\textbf{Ising}}$ to denote the same UFC as **Ising** but with the braidings defined by the antibraidings of **Ising**. It is called the time reverse of **Ising**. Both $\overline{\textbf{Ising}}$ and **Ising** $\boxtimes$ $\overline{\textbf{Ising}}$ are UMTC's. The physical meaning of this Deligne tensor product $\boxtimes$ is the stacking of the Ising topological order with its time-reversal topological order. We have **Ising** $\boxtimes$ $\overline{\textbf{Ising}} = Z(\textbf{Ising})$, where $Z(\textbf{Ising})$ is the Drinfeld center of **Ising**. We will call $Z(\textbf{Ising})$ the double Ising UMTC.

III. A GAPPABLE GAPLESS EDGE OF 2+1D $\mathbb{Z}_2$ TOPOLOGICAL ORDER

In this section, we construct a gappable nonchiral gapless edge of the $\mathbb{Z}_2$ topological order in three steps: in Sec. III A, we construct a gappable nonchiral gapless edge of the double Ising topological order after a brief review of the mathematical theory of gapless edges established in [3]; in Sec. III B, we construct a gapped domain wall between the double Ising topological order and the $\mathbb{Z}_2$ topological order; in Sec. III C, we construct a gapless edge of the $\mathbb{Z}_2$ topological order by fusing the edge in Sec. III A and the wall in Sec. III B.

A. A mathematical theory of gapless edges

In this section, we briefly review the mathematical theory gapless edges developed in [7,8]. Before we start, we briefly summarize the idea. It is well known that a gapped edge of a 2d topological order can be described by a UFC. Since the spaces of morphisms in a UFC are the finite-dimensional vector spaces of instantons, a UFC can be viewed as a category enriched in the category **H** of finite-dimensional Hilbert spaces. When the edge is gapless, the only change is that a space of morphisms becomes an infinite-dimensional space of boundary-condition changing operators in a rational conformal field theory (CFT), and can be viewed as an object

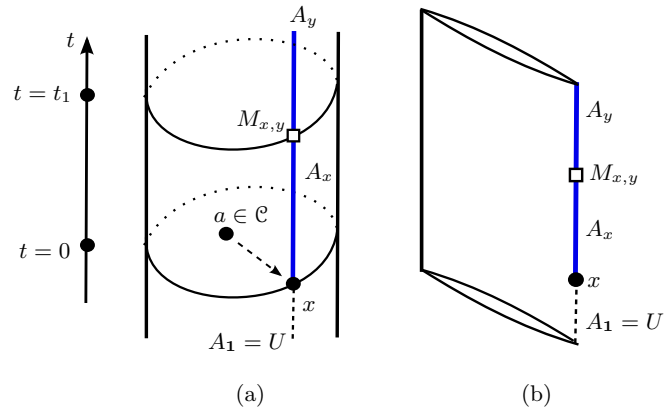

FIG. 1. The picture (a) depicts a 2d topological order $(\mathcal{C}, c)$ on a 2-disk, together with a 1d gapless edge, propagating in time. When a topological bulk excitation $a \in \mathcal{C}$ is moved to the edge at $t = 0$, it creates a topological edge excitation x or a boundary condition M_x for the OSVOA A_x living on the $t > 0$ part of the world line. At $t = t_1 > 0$, the topological edge excitation x is changed to another topological edge excitation y. This change creates a wall $M_{x,y}$ between A_x and A_y. The picture (b) depicts the quasi-(1+1)D world sheet obtained by stretching the picture (a) along the dotted arrow from a to x.

in the UMTC Mod_V of modules over a rational VOA V. As a consequence, a gapless edge can be described by a unitary fusion category enriched in Mod_V.

In Fig. 1(a), we depict a spatial two-dimensional disk propagating in time. This spatial two-dimensional disk represents a 2d topological order $(\mathcal{C}, c)$, where $\mathcal{C}$ is a unitary modular tensor category of anyons and c is the chiral central charge. If $(\mathcal{C}, c)$ is a chiral topological order, there are topologically protected gapless chiral edge modes propagating on the edge of the disk, more precisely, on the (1+1)D world sheet. It is well known that these modes are states in a chiral CFT. By the state-field correspondence in a CFT, we can also say that chiral fields propagate on the (1+1)D world sheet. In order to be monodromy free, these chiral fields can not contain any noninteger powers in the operator product expansion (OPE), thus form a so-called chiral algebra U or, equivalently, a vertex operator algebra (VOA) in the mathematical language.

The main idea of the mathematical theory of gapless edges established in [3] comes from the observation that if a bulk anyon is moved to the edge at $t = 0$, it creates a "topological edge excitation" (labeled by x) such that chiral fields living on the world line $\{t > 0\}$ supported on x [the blue line in Fig. 1(a)] are potentially different from those in U. We denote the space of all chiral fields on this world line by A_x. These chiral field can have OPE along the line but no commutativity is required. Moreover, chiral fields in A_x can have noninteger powers in their OPE. It turns out that chiral fields in A_x have to form a boundary CFT. This can be seen from Fig. 1(b), which is obtained by squeezing the solid cylinder in Fig. 1(a) to a (1+1)D world sheet. That A_x is a boundary CFT follows from the following "no-go theorem": A (1+1)D boundary-bulk conformal field theory realized by a 1d lattice Hamiltonian model with boundaries should satisfy the mathematical axioms of a boundary-bulk (or open-closed) CFT of all genera [14,15]. In other words, it should satisfy

all the modular invariant conditions and Cardy condition, etc. For this reason, the label x can also be called a *boundary condition*.[1] We denote the trivial boundary condition by $\mathbb{1}$. It is clear that $A_{\mathbb{1}} = U$. It is not hard to imagine that the boundary condition x can be change to another one y at some other point, say $t = t_1 > 0$, on the world line as depicted in Fig. 1(a). The chiral fields living on the 0D domain wall between A_x and A_y are the so-called *boundary-condition changing operators*. We denote the space of all such boundary-condition changing operators by $M_{x,y}$. It is clear that $M_{x,x} = A_x$. Boundary-condition changing operators can also have OPE, which defines a linear map

$$M_{y,z} \otimes_{\mathbb{C}} M_{x,y} \to M_{x,z}. \tag{12}$$

It was shown in [3] that $U, A_x, M_{x,y}$ should satisfy some compatibility conditions called *V-invariant boundary condition*, where V is a sub-VOA of U and will be called the *chiral symmetry* of the edge. We assume that V is unitary and rational, by which we mean that the category Mod_V of V-modules is a UMTC [16]. This V-invariant boundary condition implies that $M_{x,y}$ is a V-module, and the linear map in (12) is an intertwining operator of V or, equivalently, it defines a morphism $M_{y,z} \otimes_V M_{x,y} \to M_{x,z}$ in the category Mod_V of V-modules, where $\otimes_V$ is the tensor product in Mod_V [17]. Moreover, there is a canonical injective V-module map $\iota_x : V \hookrightarrow A_x$ for each x. Therefore, we obtain a categorical structure $\mathcal{X}^\sharp$:

(i) objects of $\mathcal{X}^\sharp$ are topological edge excitations: $x, y, z, \ldots$;

(ii) for each pair (x, y) of objects, the hom space $\hom_{\mathcal{X}^\sharp}(x, y) := M_{x,y}$ is an object in Mod_V;

(iii) there is an identity morphism $\iota_x : V = \mathbf{1}_{\mathrm{Mod}_V} \to A_x$ in Mod_V;

(iv) there is a composition morphism $M_{y,z} \otimes_V M_{x,y} \to M_{x,z}$ in Mod_V.

These satisfy some natural conditions such that $\mathcal{X}^\sharp$ is a category enriched in Mod_V or an Mod_V-enriched category. The notion of an enriched category generalizes that of a category by replacing hom-sets by hom-objects, which lives in a different category. For example, the usual notion of a category becomes a special case of a category enriched in the category of sets, and a UFC is a category enriched in **H**.

The last piece of structure is the horizontal fusion of topological edge excitations as depicted in Fig. 2, denoted by $\otimes$. It automatically provides a horizontal fusion between chiral fields in $M_{x',y'}$ and those in $M_{x,y}$ on two parallel world lines. More precisely, fusing a chiral field changing the boundary condition from x' to y' horizontally with a chiral field changing the boundary condition from x to y produces a chiral field changing the boundary condition from $x' \otimes x$ to $y' \otimes y$. As a consequence, this horizontal fusion provides

(a) a morphism $M_{x',y'} \otimes_V M_{x,y} \to M_{x'\otimes x, y'\otimes y}$ in Mod_V for objects x, y, x', y' in $\mathcal{X}^\sharp$,

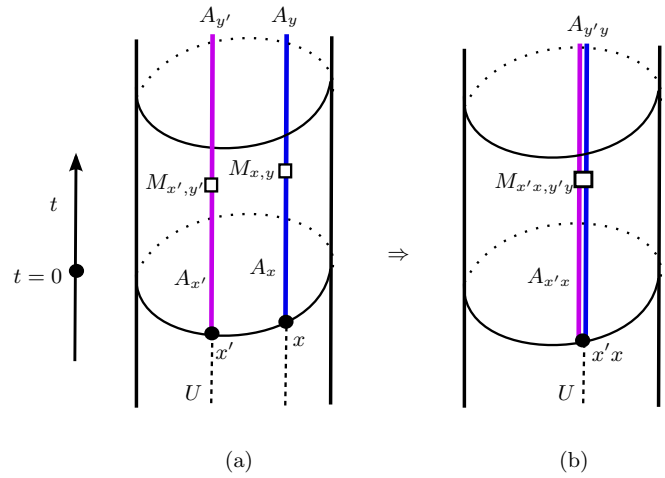

FIG. 2. This picture depicts a horizontal fusion of two boundary conditions, together with a horizontal fusion of $M_{x,y}$ and $M_{x',y'}$. For convenience, we abbreviate $x' \otimes x$ to $x'x$ in the picture.

satisfying some natural properties. It upgrades $\mathcal{X}^\sharp$ to an Mod_V-enriched monoidal category [2]. We denote this gapless edge by a pair $(V, \mathcal{X}^\sharp)$.

Theorem 1 ([18]). There is a braided equivalence $\mathcal{C} \simeq Z(\mathcal{X}^\sharp)$, where $Z(\mathcal{X}^\sharp)$ is the monoidal center of $\mathcal{X}^\sharp$ introduced in [18].

Remark 6. This theorem says that all boundaries, regardless gapped or gapless, all share the same bulk as their mathematical centers. By [8], these boundaries are all spatially Morita equivalent, and their center is precisely the only invariant of this spatial Morita equivalence class. Ji and Wen proposed that the UMTC $\mathcal{C}$ associated to the bulk should be viewed as a "categorical symmetry" of all boundaries in [19]. This idea is further developed in [20].

Example 3. The well-known Ising 2d topological order can be described by a pair $(\mathbf{Ising}, \frac{1}{2})$, where **Ising** denotes the Ising UMTC and $\frac{1}{2}$ is the chiral central charge. It has a canonical chiral gapless edge described by a pair $(V, \mathbf{Ising}^\sharp)$, where we note the following:

(a) V is the Ising VOA of the central charge $c = \frac{1}{2}$ and $\mathrm{Mod}_V = \mathbf{Ising}$.

(b) $\mathbf{Ising}^\sharp$ is the **Ising**-enriched fusion category (i.e., **Ising** enriched in itself) defined as follows:

(1) objects in $\mathbf{Ising}^\sharp$ are the same as objects in **Ising**, i.e., $x = \mathbf{1}, \psi, \sigma$ and their direct sums;

(2) for $x, y \in \mathbf{Ising}$, we have the hom space defined by $\hom_{\mathbf{Ising}^\sharp}(x, y) := M_{x,y} = y \otimes x^*$;

(3) the identity morphism is defined by $\mathbf{1} \xrightarrow{u_x} x \otimes x^* = M_{x,x}$;

(4) the composition morphism $M_{y,z} \otimes M_{x,y} \xrightarrow{\circ} M_{x,z}$ is defined by $z \otimes y^* \otimes y \otimes x^* \xrightarrow{1\otimes v_y \otimes 1} z \otimes x^*$;

(5) a fusion product between two objects is the same as the one in **Ising**; the fusion product on hom space is a morphism $M_{x',y'} \otimes M_{x,y} \to M_{x'\otimes x, y'\otimes y}$ defined by

$$y' \otimes x'^* \otimes y \otimes x^* \xrightarrow{1\otimes b_{x'^*, y\otimes x^*}} (y' \otimes y) \otimes (x' \otimes x)^*.$$

[1] Actually, the category of topological edge excitations is closely related to but slightly different from that of boundary conditions (for boundary CFT's) in general (see [7]). In the case studied in this work, two categories coincide.

The enriched monoidal category $\mathbf{Ising}^\sharp$ is a special case of the standard construction given by Morrison and Penneys in [2]. We recall this construction only in a special setting. Let $\mathcal{B}$ be a braided fusion category and $\overline{\mathcal{B}}$ its time reversal. Let $\mathcal{M}$ be a fusion category and $Z(\mathcal{M})$ its Drinfeld center. Let $F : \overline{\mathcal{B}} \to Z(\mathcal{M})$ be a braided monoidal functor. Then, we have a functor $\odot : \overline{\mathcal{B}} \times \mathcal{M} \to \mathcal{M}$ defined by the composition of the following functors:

$$\overline{\mathcal{B}} \times \mathcal{M} \xrightarrow{F\times \mathrm{id}_{\mathcal{M}}} Z(\mathcal{M}) \times \mathcal{M} \xrightarrow{\mathrm{forget}\times \mathrm{id}_{\mathcal{M}}} \mathcal{M} \times \mathcal{M} \xrightarrow{\otimes} \mathcal{M},$$

where forget : $Z(\mathcal{M}) \to \mathcal{M}$ is the forgetful functor (by forgetting the half-braidings). There is a canonical construction of a $\mathcal{B}$-enriched monoidal category $\mathcal{M}^\sharp$ from the pair $(\mathcal{B}, \mathcal{M})$, where objects in $\mathcal{M}^\sharp$ are objects in $\mathcal{M}$, and for $x, y \in \mathcal{M}$, $\hom_{\mathcal{M}^\sharp}(x, y)$ is defined by the so-called internal hom $[x, y]$ in $\overline{\mathcal{B}}$ (or in $\mathcal{B}$). More precisely, $[x, y]$ is uniquely determined by the following adjunction relation:

$$\hom_{\mathcal{M}}(b \odot x, y) \simeq \hom_{\mathcal{B}}(b, [x, y]), \quad \forall\, b \in \mathcal{B}. \tag{13}$$

For convenience, we simply denote $\mathcal{M}^\sharp$ by the pair $(\mathcal{B}, \mathcal{M})$. Such a $\mathcal{B}$-enriched monoidal category will be called a $\mathcal{B}$-enriched fusion category.

Note that $\mathbf{Ising}^\sharp = (\mathbf{Ising}, \mathbf{Ising})$ is an **Ising**-enriched fusion category, and $M_{x,y} = y \otimes x^*$ is the internal hom $[x, y]$ because $[x, y] = y \otimes x^*$ is clearly a solution to the the adjunction "equation" (13) when $\mathcal{M} = \mathcal{B} = \mathbf{Ising}$. Therefore, we denote $(V, \mathbf{Ising}^\sharp)$ by the triple $(V, \mathbf{Ising}, \mathbf{Ising})$.

The mathematical theory of nonchiral gapless edges is similar. We do not give a review of this theory (see [8] for more details). Instead, we give an example of gappable nonchiral gapless edge.

Example 4. By folding an Ising topological order $(\mathbf{Ising}, \frac{1}{2})$ with the canonical chiral gapless edge, we obtain a double Ising topological order $(\mathbf{Ising} \boxtimes \overline{\mathbf{Ising}}, 0)$ equipped with both chiral gapless edge modes described by $(V, \mathbf{Ising}, \mathbf{Ising})$ and antichiral gapless edge modes described by $(\overline{V}, \overline{\mathbf{Ising}}, \overline{\mathbf{Ising}})$, where $\overline{V}$ is the same VOA as V but contains only antichiral fields $\phi(\bar{z}), \forall\, \phi \in V$. Altogether, they form a nonchiral gapless edge of the double Ising topological order $(\mathbf{Ising} \boxtimes \overline{\mathbf{Ising}}, 0)$ described by the triple

$$(V \otimes_{\mathbb{C}} \overline{V},\ \mathbf{Ising} \boxtimes \overline{\mathbf{Ising}},\ \mathbf{Ising} \boxtimes \overline{\mathbf{Ising}}). \tag{14}$$

In this nonchiral case, $V \otimes_{\mathbb{C}} \overline{V}$ is called the nonchiral symmetry of the edge. It is not a VOA. It contains both the chiral part and the antichiral part, and is called a full field algebra in mathematics [21]. This nonchiral gapless edge is clearly gappable.

Remark 7. We briefly outline the mathematical theory of gapless edges of 2d topological orders. Intrigued readers can consult with [7,8] for more details, and for what types of questions this theory is capable of answering, and for applications in higher dimensions.

B. A gapped wall between double Ising and toric code

It was first shown by Bais and Slingerland in [22] on a physical level of rigor that one can obtain the $\mathbb{Z}_2$ topological order from the double Ising via an anyon condensation. In this section, we will give a complete and rigorous derivation of this result based on the mathematical theory of anyon condensation developed in [5]. As a by-product, we construct a gapped domain wall between the double Ising and the $\mathbb{Z}_2$ topological orders.

An anyon condensation from an old topological order $(\mathcal{C}, c)$ to a new phase $(\mathcal{D}, c)$ is controlled by a condensable algebra A in $\mathcal{C}$. We recall this notion below.

Definition 1. Let $\mathcal{C}$ be a UMTC. An algebra A in $\mathcal{C}$ is a triple (A, μ, ι), where A is an object in $\mathcal{C}$, $\mu : A \otimes A \to A$ and $\iota : \mathbf{1} \to A$ are morphisms satisfying the following conditions:

$$\mu \circ (\mu \otimes \mathrm{id}_A) \circ \alpha_{A,A,A} = \mu \circ (\mathrm{id}_A \otimes \mu),$$

$$\mu \circ (\iota \otimes \mathrm{id}_A) = \mathrm{id}_A = \mu \circ (\mathrm{id}_A \otimes \iota).$$

The algebra A is called commutative if $\mu = \mu \circ b_{A,A}$, where $A \otimes A \xrightarrow{b_{A,A}} A \otimes A$ is the braiding isomorphism.

Definition 2. A right A-module in $\mathcal{C}$ is a pair (M, μ_M), where M is an object in $\mathcal{C}$ and $\mu_M : M \otimes A \to M$ is such that

$$\mu_M \circ (\mathrm{id}_M \otimes \mu) = \mu_M \circ (\mu_M \otimes \mathrm{id}_A) \circ \alpha_{M,A,A},$$
$$\mu_M \circ (\mathrm{id}_M \otimes \iota) = \mathrm{id}_M.$$

We denote the category of right A-modules in $\mathcal{C}$ by $\mathcal{C}_A$. A right A-module is called a *local A-module* if $\mu_M \circ b_{A,M} \circ b_{M,A} = \mu_M$. We denote the category of local A-modules in $\mathcal{C}$ by $\mathcal{C}_A^0$, which is a full subcategory of $\mathcal{C}_A$.

Definition 3. An algebra (A, μ, ι) is called *separable* if $\mu : A \otimes A \to A$ splits as a morphism of A-A-bimodule. Namely, there is an A-A-bimodule map $e : A \to A \otimes A$ such that $\mu \circ e = \mathrm{id}_A$. A separable algebra is called *connected* if $\dim \hom_{\mathcal{C}}(\mathbf{1}, A) = 1$. We will call a connected commutative separable algebra as a *condensable algebra*. A condensable algebra A is called *Lagrangian* if $\dim(A)^2 = \dim(\mathcal{C})$.

If A is condensable, the category $\mathcal{C}_A$ is a UFC. Its full subcategory $\mathcal{C}_A^0$ is a UMTC with the braidings, rigidity, and spins inherited from those in $\mathcal{C}$. In particular, for a local A-module $\hat{M} = (M, \mu_{\hat{M}})$, the spin (or twist) $\theta_{\hat{M}}^A$ in $\mathcal{C}_A^0$ is defined by θ_M in $\mathcal{C}$. Moreover, we have the following identities [23]:

$$\begin{aligned} \dim(\mathcal{C}_A) &= \frac{\dim(\mathcal{C})}{\dim(A)}, \\ \dim(\mathcal{C}_A^0) &= \frac{\dim(\mathcal{C})}{\dim(A)^2}, \\ \dim_A(x) &= \frac{\dim x}{\dim A}, \end{aligned} \tag{15}$$

where $\dim x$ is the quantum dimension of x in $\mathcal{C}$ and $\dim_A(x)$ is that of x in $\mathcal{C}_A$. If, in addition, A is Lagrangian, we have $\mathcal{C}_A^0 = \mathbf{H}$.

Example 5. There are two condensable algebras in **Toric**: $A_e = \mathbf{1} \oplus e$ and $A_m = \mathbf{1} \oplus m$. Both of them are Lagrangian.

Example 6. Since a condensable algebra A satisfies $\theta_A = \mathrm{id}_A$, the only condensable algebra A in **Ising** is $\mathbf{1}$.

Example 7. Let $Z(\mathbf{Ising}) = \mathbf{Ising} \boxtimes \overline{\mathbf{Ising}} \xrightarrow{\otimes} \mathbf{Ising}$ be the tensor product functor and let $R : \mathbf{Ising} \to Z(\mathbf{Ising})$ be its right adjoint functor.

(1) The following object

$$R(\mathbf{1}) = \oplus_{i \in \mathrm{Irr}(\mathbf{Ising})} i^* \boxtimes i = \mathbf{1} \boxtimes \mathbf{1} \oplus \psi \boxtimes \psi \oplus \sigma \boxtimes \sigma \tag{16}$$

has the structure of a Lagrangian algebra naturally induced from the algebraic structure on $\mathbf{1}$ and, at the same time, describes a modular invariant closed CFT ([24], Theorem 3.4). More explicitly, the multiplication map (or the structure constants of the closed CFT) $m : R(\mathbf{1}) \otimes R(\mathbf{1}) \to R(\mathbf{1})$ was defined by (first appeared in [25,26], we take it from ([24], Eqs. (2.17) and (2.55))

$$m = \bigoplus_{i,j,k\in \mathrm{Irr}(\mathbf{Ising})} \sum_{\alpha}$$

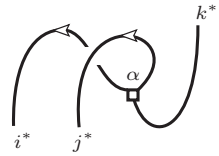

$\boxtimes$

, (17)

where α labels both the basis of $\hom_{\mathbf{Ising}}(i \otimes j, k)$ and the dual basis of $\hom_{\mathbf{Ising}}(k, i \otimes j)$ [recall Eqs. (7) and (6)]. The unit map is defined by the canonical embedding $\mathbf{1}_{Z(\mathbf{Ising})} \hookrightarrow R(\mathbf{1})$.

(2) We denote the fusion subcategory of **Ising** consisting of $\mathbf{1}$ and ψ by $\mathcal{A}$. Then, $\mathcal{A} \boxtimes \overline{\mathcal{A}}$ is a fusion subcategory of $Z(\mathbf{Ising})$. We have a subalgebra A of $R(\mathbf{1})$ defined by

$$A := R(\mathbf{1}) \cap (\mathcal{A} \boxtimes \overline{\mathcal{A}}) = \mathbf{1} \boxtimes \mathbf{1} \oplus \psi \boxtimes \psi \tag{18}$$

which is also a condensable algebra in $\mathcal{A} \boxtimes \overline{\mathcal{A}}$. More explicitly, using the right unit isomorphisms $r_{\mathbf{1}} : \mathbf{1} \otimes \mathbf{1} \simeq \mathbf{1}$, $r_\psi : \psi \otimes \mathbf{1} \simeq \psi$ and the duality map v_ψ [recall (4)], we can rewrite the multiplication map m in (17) as follows:

$$\begin{aligned} m = {} & (\mathbf{1} \otimes \mathbf{1} \xrightarrow{r_{\mathbf{1}}} \mathbf{1}) \boxtimes (\mathbf{1} \otimes \mathbf{1} \xrightarrow{r_{\mathbf{1}}} \mathbf{1}) \\ & \oplus (\mathbf{1} \otimes \psi \xrightarrow{r_\psi} \psi) \boxtimes (\mathbf{1} \otimes \psi \xrightarrow{r_\psi} \psi) \\ & \oplus (\psi \otimes \mathbf{1} \xrightarrow{r_\psi} \psi) \boxtimes (\psi \otimes \mathbf{1} \xrightarrow{r_\psi} \psi) \\ & \oplus (\psi \otimes \psi \xrightarrow{-v_\psi} \mathbf{1}) \boxtimes (\psi \otimes \psi \xrightarrow{v_\psi} \mathbf{1}). \end{aligned}$$

Note that $\dim A = 2$.

According to the anyon condensation theory [5], by condensing the condensable algebra A in the initial phase $(Z(\mathbf{Ising}), 0)$, we obtain

(1) a new 2d topological order $(Z(\mathbf{Ising})^0_A, 0)$, where $Z(\mathbf{Ising})^0_A$ denotes the category of local A-modules in $Z(\mathbf{Ising})$ (recall Definition 2).

(2) and a 1d gapped domain wall described by the UFC $Z(\mathbf{Ising})_A$, where $Z(\mathbf{Ising})_A$ denotes the category of right A-modules in $Z(\mathbf{Ising})$ (recall Definition 2).

Our goal is to work out these two categories $Z(\mathbf{Ising})_A$ and $Z(\mathbf{Ising})^0_A$ explicitly and prove that $Z(\mathbf{Ising})^0_A \simeq \mathbf{Toric}$ as UMTC's. Before we do that, we first collect a few relevant results.

(1) Notice that we have

$$\begin{aligned} \dim Z(\mathbf{Ising})_A &= \frac{Z(\mathbf{Ising})}{\dim A} = 8, \\ \dim Z(\mathbf{Ising})^0_A &= \frac{Z(\mathbf{Ising})}{(\dim A)^2} = \frac{16}{2^2} = 4. \end{aligned} \tag{19}$$

(2) A is clearly a simple right A-module and a local A-module.

(3) Another obvious simple right A-module is $(\sigma \boxtimes \sigma)$ because the following splitting

$$R(\mathbf{1}) = A \oplus (\sigma \boxtimes \sigma)$$

is a splitting of A-A-bimodules because A is separable. The right A-module structure on $(\sigma \boxtimes \sigma)$ (recall Definition 2) can be explicitly defined by [recall Eq. (7)]

$$\begin{aligned} \mu_{\sigma\boxtimes\sigma} := {} & (\sigma \otimes \mathbf{1} \xrightarrow{r_\sigma} \sigma) \boxtimes (\sigma \otimes \mathbf{1} \xrightarrow{r_\sigma} \sigma) \\ & \oplus \left(\sigma \otimes \psi \xrightarrow{\lambda^\sigma_{\sigma\psi}} \sigma\right) \boxtimes \left(\sigma \otimes \psi \xrightarrow{\lambda^\sigma_{\sigma\psi}} \sigma\right). \end{aligned} \tag{20}$$

Using Eq. (11), it is easy to see that $\sigma \boxtimes \sigma$ is a local A-module.

(4) The condensable algebra A has a nontrivial algebraic automorphism defined by

$$\delta : A = (\mathbf{1} \boxtimes \mathbf{1}) \oplus (\psi \boxtimes \psi) \xrightarrow{1\oplus -1} (\mathbf{1} \boxtimes \mathbf{1}) \oplus (\psi \boxtimes \psi) = A.$$

And δ is an involution, i.e., $\delta^2 = \mathrm{id}_A$.

(5) We can use δ to twist the A-action on a right A-module $M = (M, \mu_M)$ and obtain a new right A-module structure, denoted by M^{tw}, with a new action defined by

$$M \otimes A \xrightarrow{\mathrm{id}_M \otimes \delta} M \otimes A \xrightarrow{\mu_M} M.$$

(a) If $M = x \otimes A$ for $x \in \mathcal{C}$ with the right A-action defined

$$x \otimes A \otimes A \xrightarrow{1\otimes\mu} x \otimes A, \tag{21}$$

then we have $(x \otimes A) \simeq (x \otimes A)^{\mathrm{tw}}$ as right A-modules with the isomorphism given by $x \otimes A \xrightarrow{\mathrm{id}_x \otimes \delta} x \otimes A$.

(b) For $M = (\sigma \boxtimes \sigma)$, we obtain a new local A-module $(\sigma \boxtimes \sigma)^{\mathrm{tw}}$ defined by [recall Eq. (7)]

$$\begin{aligned} \mu_{(\sigma\boxtimes\sigma)^{\mathrm{tw}}} := {} & (\sigma \otimes \mathbf{1} \xrightarrow{r_\sigma} \sigma) \boxtimes (\sigma \otimes \mathbf{1} \xrightarrow{r_\sigma} \sigma) \\ & \oplus \left(\sigma \otimes \psi \xrightarrow{-\lambda^\sigma_{\sigma\psi}} \sigma\right) \boxtimes \left(\sigma \otimes \psi \xrightarrow{\lambda^\sigma_{\sigma\psi}} \sigma\right). \end{aligned}$$

It is clear that $(\sigma \boxtimes \sigma)^{\mathrm{tw}}$ is not isomorphic to $(\sigma \boxtimes \sigma)$ as local A-modules.

We need to find all right A-modules. We use the fact that all simple objects in $Z(\mathbf{Ising})_A$ can be realized by a direct summand of $x \otimes A$ for $x \in \mathrm{Irr}(Z(\mathbf{Ising}))$ with the right A-action defined by (21) because $x \simeq x \otimes_A A$ and A is separable. Therefore, we obtain a complete list of simple right A-modules as follows:

(1) $(\mathbf{1} \boxtimes \mathbf{1}) \otimes A = A$.

(2) $(\psi \boxtimes \mathbf{1}) \otimes A = \psi \boxtimes \mathbf{1} \oplus \mathbf{1} \boxtimes \psi$ is clearly a simple local A-module. It is useful to write the right A-action on $\psi \boxtimes \mathbf{1} \oplus \mathbf{1} \boxtimes \psi$ explicitly as follows:

$$(r_\psi \boxtimes r_{\mathbf{1}}) \oplus (v_\psi \boxtimes l_\psi) \oplus (r_{\mathbf{1}} \boxtimes r_\psi) \oplus (-l_\psi \boxtimes v_\psi). \tag{22}$$

(3) $(\mathbf{1} \boxtimes \psi) \otimes A = \psi \boxtimes \mathbf{1} \oplus \mathbf{1} \boxtimes \psi$ is a simple local A-module. It is useful to write the right A-action on $\psi \boxtimes \mathbf{1} \oplus \mathbf{1} \boxtimes \psi$ explicitly as follows:

$$(r_\psi \boxtimes r_{\mathbf{1}}) \oplus (-v_\psi \boxtimes l_\psi) \oplus (r_{\mathbf{1}} \boxtimes r_\psi) \oplus (l_\psi \boxtimes v_\psi). \tag{23}$$

Using the explicit right A-actions given in Eqs. (22) and (23), it is obvious to see that

$$(\mathbf{1} \boxtimes \psi) \otimes A = ((\psi \boxtimes \mathbf{1}) \otimes A)^{\mathrm{tw}} \simeq (\psi \boxtimes \mathbf{1}) \otimes A$$

as right A-modules.

(4) $(\psi \boxtimes \psi) \otimes A$ is a simple local A-module. By writing out the right A-action on $\mathbf{1} \boxtimes \mathbf{1} \oplus \psi \boxtimes \psi$ in basis explicitly

and comparing it with Eq. (20), we see that $(\psi \boxtimes \psi) \otimes A = A^{\mathrm{tw}} \simeq A$.

(5) $(\sigma \boxtimes \sigma) \otimes A$ is a local A-module but not simple. By checking the right A-action in basis, we obtain that

$$(\sigma \boxtimes \sigma) \otimes A \simeq (\sigma \boxtimes \sigma) \oplus (\sigma \boxtimes \sigma)^{\mathrm{tw}}$$

as local A-modules.

(6) $(\sigma \boxtimes \mathbf{1}) \otimes A = (\sigma \boxtimes \mathbf{1}) \oplus (\sigma \boxtimes \psi)$ is a simple right A-module but not local.

(7) $(\sigma \boxtimes \psi) \otimes A = (\sigma \boxtimes \mathbf{1}) \oplus (\sigma \boxtimes \psi)$ is a simple right A-module but not local. By writing out the right A-action on $(\sigma \boxtimes \mathbf{1}) \oplus (\sigma \boxtimes \psi)$ in basis explicitly for both cases 6 and 7, one see that $(\sigma \boxtimes \psi) \otimes A = ((\sigma \boxtimes \mathbf{1}) \otimes A)^{\mathrm{tw}} \simeq (\sigma \boxtimes \mathbf{1}) \otimes A$.

(8) $(\mathbf{1} \boxtimes \sigma) \otimes A = (\mathbf{1} \boxtimes \sigma) \oplus (\psi \boxtimes \sigma)$ is a simple right A-module but not local.

(9) $(\psi \boxtimes \sigma) \otimes A = (\mathbf{1} \boxtimes \sigma) \oplus (\psi \boxtimes \sigma)$ is a simple right A-module but not local. By writing out the right A-action on $(\mathbf{1} \boxtimes \sigma) \oplus (\psi \boxtimes \sigma)$ in basis explicitly for both cases 8 and 9, one can see that $(\psi \boxtimes \sigma) \otimes A = ((\mathbf{1} \boxtimes \sigma) \otimes A)^{\mathrm{tw}} \simeq (\sigma \boxtimes \mathbf{1}) \otimes A)$.

To summarize, we have found all simple objects in $Z(\mathbf{Ising})_A$:

(i) Four simple local A-modules with new and shorter notations

$$\begin{aligned} &\mathbb{1} := A = (\mathbf{1} \boxtimes \mathbf{1}) \oplus (\psi \boxtimes \psi), \quad e := (\sigma \boxtimes \sigma), \\ &m := (\sigma \boxtimes \sigma)^{\mathrm{tw}}, \\ &f := (\psi \boxtimes \mathbf{1}) \otimes A = \psi \boxtimes \mathbf{1} \oplus \mathbf{1} \boxtimes \psi \end{aligned} \tag{24}$$

with quantum dimensions in $Z(\mathbf{Ising})_A$ all given by 1.

(ii) Two simple nonlocal right A-modules with new and shorter notations

$$\begin{aligned} \chi_+ &:= (\mathbf{1} \boxtimes \sigma) \otimes A = (\mathbf{1} \boxtimes \sigma) \oplus (\psi \boxtimes \sigma), \\ \chi_- &:= (\sigma \boxtimes \mathbf{1}) \otimes A = (\sigma \boxtimes \mathbf{1}) \oplus (\sigma \boxtimes \psi) \end{aligned} \tag{25}$$

with quantum dimensions in $Z(\mathbf{Ising})_A$ both given by $\sqrt{2}$.

Remark 8. One can also check directly from the sum of quantum dimensions and Eq. (19) to see that we have found all simple right A-modules and all simple local A-modules.

Now, we work out the fusion rules of $Z(\mathbf{Ising})_A^0$. Note that the fusion product in $Z(\mathbf{Ising})_A^0$ is given by the relative tensor product $\otimes_A$. In order to see how $Z(\mathbf{Ising})_A^0$ can be identified with the UMTC **Toric** as an abstract tensor category. We adopt the new convention of notation as illustrated by the following examples:

$$\begin{aligned} e \star m &:= (\sigma \boxtimes \sigma) \otimes_A (\sigma \boxtimes \sigma)^{\mathrm{tw}}, \\ \chi_+ \star f &:= [(\mathbf{1} \boxtimes \sigma) \otimes A] \otimes_A [(\psi \boxtimes \mathbf{1}) \otimes A], \end{aligned}$$

where we have also replaced the tensor product $\otimes_A$ in $Z(\mathbf{Ising})_A$ by $\star$.

(1) The right A-module structure on $(\sigma \boxtimes \sigma)$ gives a left A-module structure on $(\sigma \boxtimes \sigma)^* = (\sigma \boxtimes \sigma)$. One can check that it coincides with the left A-module structure on $(\sigma \boxtimes \sigma)$ defined by

$$A \otimes (\sigma \boxtimes \sigma) \xrightarrow{b_{A,\sigma\boxtimes\sigma}} (\sigma \boxtimes \sigma) \otimes A \to A.$$

As a consequence, the dual of $(\sigma \boxtimes \sigma)$ in $Z(\mathbf{Ising})_A^0$ is precisely $(\sigma \boxtimes \sigma)$. In other words, we must have $(\sigma \boxtimes \sigma) \otimes_A (\sigma \boxtimes \sigma) \simeq A$ as right A-modules.

(2) Similarly, we have $(\sigma \boxtimes \sigma)^{\mathrm{tw}} \otimes_A (\sigma \boxtimes \sigma)^{\mathrm{tw}} \simeq A$ as right A-modules.

(3) On the one hand, we have

$$\begin{aligned} &[(\sigma \boxtimes \sigma) \otimes A] \otimes_A (\sigma \boxtimes \sigma) \\ &\quad \simeq [(\sigma \boxtimes \sigma) \oplus (\sigma \boxtimes \sigma)^{\mathrm{tw}}] \otimes_A (\sigma \boxtimes \sigma). \end{aligned}$$

On the other hand, we have

$$\begin{aligned} [(\sigma \boxtimes \sigma) \otimes A] \otimes_A (\sigma \boxtimes \sigma) &\simeq (\sigma \boxtimes \sigma) \otimes (\sigma \boxtimes \sigma) \\ &\simeq (\mathbf{1} \oplus \psi) \boxtimes (\mathbf{1} \oplus \psi) \\ &\simeq A \oplus [(\psi \boxtimes \mathbf{1}) \oplus (\mathbf{1} \boxtimes \psi)]. \end{aligned}$$

Therefore, we obtain $(\sigma \boxtimes \sigma)^{\mathrm{tw}} \otimes_A (\sigma \boxtimes \sigma) \simeq (\psi \boxtimes \mathbf{1}) \otimes A$ as right A-modules.

As a consequence, we obtain the following fusion rules of $Z(\mathbf{Ising})_A^0$:

$$\mathbb{1} \star x = x, \quad e \star e = m \star m = f \star f = \mathbb{1}, \quad e \star m = f, \tag{26}$$

where $x = \mathbb{1}, e, m, f$.

Note that this fusion rule coincides with that of **Toric**. According to [27], there are exactly two modular tensor categories that share these fusion rules. They are **Toric** and $\mathrm{Spin}(8)_1$, the spins of which are given by $(1, 1, 1, -1)$ and $(1, -1, -1, -1)$, respectively. In our case, we have

$$\theta_e^A = \theta_m^A = \theta_\sigma \theta_\sigma^{-1} = 1, \qquad \theta_f^A = \theta_\psi = -1,$$

where θ_-^A denotes the spins in $Z(\mathbf{Ising})_A^0$. Therefore, we have proved the following result.

Theorem 2. $Z(\mathbf{Ising})_A^0 \simeq$ **Toric** as UMTC's.

It is useful to work out the remaining fusion rules in $Z(\mathbf{Ising})_A$ as follows:

$$\begin{aligned} &\chi_\pm \star \chi_\pm = \mathbb{1} \oplus f, \qquad \chi_\pm \star \chi_\mp = e \oplus m, \\ &e \star \chi_\pm = \chi_\pm \star e = m \star \chi_\pm = \chi_\pm \star m = \chi_\mp. \end{aligned} \tag{27}$$

We give a proof below:

(1) $\chi_+ \star \chi_+ = [(\mathbf{1} \boxtimes \sigma) \otimes A] \otimes_A [(\mathbf{1} \boxtimes \sigma) \otimes A] \simeq (\mathbf{1} \boxtimes \sigma) \otimes (\mathbf{1} \boxtimes \sigma) \otimes A \simeq A \oplus (\mathbf{1} \boxtimes \psi) \otimes A = \mathbb{1} \oplus f$.

(2) $\chi_- \star \chi_- = [(\sigma \boxtimes \mathbf{1}) \otimes A] \otimes_A [(\sigma \boxtimes \mathbf{1}) \otimes A] \simeq (\sigma \boxtimes \mathbf{1}) \otimes (\sigma \boxtimes \mathbf{1}) \otimes A \simeq A \oplus (\psi \boxtimes \mathbf{1}) \otimes A = \mathbb{1} \oplus f$.

(3) $\chi_+ \star \chi_- = [(\mathbf{1} \boxtimes \sigma) \otimes A] \otimes_A [(\sigma \boxtimes \mathbf{1}) \otimes A] \simeq (\sigma \boxtimes \sigma) \otimes A = e \oplus m = \chi_- \star \chi_+$.

(4) $e \star \chi_+ \simeq \chi_+ \star e = [(\mathbf{1} \boxtimes \sigma) \otimes A] \otimes_A (\sigma \boxtimes \sigma) \simeq \sigma \boxtimes (\mathbf{1} \oplus \psi) = \chi_-$.

(5) $e \star \chi_- \simeq \chi_- \star e = [(\sigma \boxtimes \mathbf{1}) \otimes A] \otimes_A (\sigma \boxtimes \sigma) \simeq (\mathbf{1} \oplus \psi) \boxtimes \sigma = \chi_+$.

(6) $m \star \chi_+ \simeq \chi_+ \star m = [(\mathbf{1} \boxtimes \sigma) \otimes A] \otimes_A (\sigma \boxtimes \sigma)^{\mathrm{tw}} \simeq \chi_-$.

(7) $m \star \chi_- \simeq \chi_- \star m = [(\sigma \boxtimes \mathbf{1}) \otimes A] \otimes_A (\sigma \boxtimes \sigma)^{\mathrm{tw}} \simeq \chi_+$.

Remark 9. From the above identities, one can see that $x = x^*$ and $x \star y = y \star x$ as objects for all $x \in Z(\mathbf{Ising})_A$.

In summary, by condensing A in the double Ising topological order $(Z(\mathbf{Ising}), 0)$, we obtain the 2d $\mathbb{Z}_2$ topological order and a gapped domain wall given by the UFC $Z(\mathbf{Ising})_A$, which consists of six simple wall excitations $\mathbb{1}, e, m, f, \chi_\pm$.

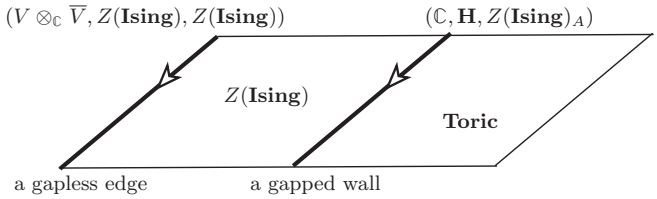

FIG. 3. This picture depicts a gapped domain wall between the double Ising and the $\mathbb{Z}_2$ topological order, and a gapless edge of the double Ising topological order.

C. First gappable nonchiral gapless edge

In this section, we combine results in Secs. III A and III B to construct a gappable nonchiral gapless edge of the $\mathbb{Z}_2$ topological order. In Example 4, we have constructed a gappable nonchiral gapless edge of the double Ising topological order. It can be expressed by a triple

$$(V \otimes_{\mathbb{C}} \overline{V},\ Z(\mathbf{Ising}),\ Z(\mathbf{Ising})). \tag{28}$$

In Sec. III B, we have constructed a gapped domain wall $Z(\mathbf{Ising})_A$ between the double Ising and the $\mathbb{Z}_2$ topological orders. Using the notion of enriched fusion category introduced in Sec. III A, the UFC $Z(\mathbf{Ising})_A$ can also be viewed as an enriched fusion category determined by the pair $(\mathbf{H}, Z(\mathbf{Ising})_A)$. Therefore, this gapped domain wall can also be expressed as a triple

$$(\mathbb{C},\ \mathbf{H},\ Z(\mathbf{Ising})_A), \tag{29}$$

where the complex numbers $\mathbb{C}$ should be viewed as the trivial VOA of central charge 0.

By fusing the gapless edge (28) and the gapped domain wall (29) as depicted in Fig. 3, we obtain a nonchiral gapless edge of the $\mathbb{Z}_2$ topological order. Using the fusion product defined in ([3], Eq. (5.2)), this gapless edge is given by the following triples:

$$\begin{aligned}(V \otimes_{\mathbb{C}} \overline{V},\ Z(\mathbf{Ising}),\ Z(\mathbf{Ising})) \boxtimes_{(Z(\mathbf{Ising}),0)} (\mathbb{C},\ \mathbf{H},\ Z(\mathbf{Ising})_A) &= (V \otimes_{\mathbb{C}} \overline{V} \otimes_{\mathbb{C}} \mathbb{C},\ Z(\mathbf{Ising}) \boxtimes \mathbf{H},\ Z(\mathbf{Ising}) \boxtimes_{Z(\mathbf{Ising})} Z(\mathbf{Ising})_A) \\ &= (V \otimes_{\mathbb{C}} \overline{V},\ Z(\mathbf{Ising}),\ Z(\mathbf{Ising})_A).\end{aligned} \tag{30}$$

The validity of this fusion formula is explained in details in [7]. We can describe the observables on this gapless edge $(V \otimes_{\mathbb{C}} \overline{V},\ Z(\mathbf{Ising}),\ Z(\mathbf{Ising})_A)$ explicitly as follows:

(i) $V \otimes_{\mathbb{C}} \overline{V}$ is the nonchiral symmetry.

(ii) Topological edge excitations (or boundary conditions) on this gapless edge are objects in $Z(\mathbf{Ising})_A$. In particular, there are exactly six simple ones: $\mathbb{1}, e, m, f, \chi_\pm$. They can be fused horizontally according to the fusion rules in $Z(\mathbf{Ising})_A$ [see Eqs. (26) and (27)].

(iii) Boundary CFT's and walls between them $M_{x,y}$ are given by internal homs $[x, y] = (x \otimes_A y^*)^*$ [28]. We want to work out each $[x, y]$ as objects in order to compare them with the partition functions obtained in lattice model realizations in Sec. IV. Recall that $x^* = x$ for $x \in Z(\mathbf{Ising})_A$. Moreover, for $x, y = \mathbb{1}, e, m, f, \chi_\pm$, we obtain

$$M_{x,y} = [x, y] = [\mathbb{1}, x \otimes_A y] = x \otimes_A y, \quad \text{as objects.} \tag{31}$$

Each x is defined by objects in $Z(\mathbf{Ising})$ by Eqs. (24) and (25).

This nonchiral gapless edge is clearly gappable.

D. Partition functions of $M_{x,y}$ in the first edge

Recall that the 2d $\mathbb{Z}_2$ topological order has two gapped edges. One is obtained by condensing m particles and the other by condensing e particles [10]. Both gapped edges can be described by the same UFC $\mathcal{R}\mathrm{ep}(\mathbb{Z}_2)$ but equipped with two different bulk-to-edge functors $\mathbf{Toric} \to \mathcal{R}\mathrm{ep}(\mathbb{Z}_2)$, corresponding to different condensations. The bulk-edge correspondence says that the Drinfeld center of $\mathcal{R}\mathrm{ep}(\mathbb{Z}_2)$ gives the bulk, i.e., bulk = the center of the edge. A purely edge topological phase transition between these two gapped edges closes the gap and produces a gappable gapless edge at the critical point. Since the bulk-edge correspondence holds before and after the transition, we expect that it holds at the critical point as well.

In Sec. III C, we have constructed a gappable gapless edge $(V \otimes_{\mathbb{C}} \overline{V},\ Z(\mathbf{Ising}),\ Z(\mathbf{Ising})_A)$ of the 2d $\mathbb{Z}_2$ topological order. It shares the same bulk with the two gapped edges. Mathematically, it is because the enriched fusion category $(Z(\mathbf{Ising}),\ Z(\mathbf{Ising})_A)$ and the UFC $\mathcal{R}\mathrm{ep}(\mathbb{Z}_2)$ share the same Drinfeld center [18] or, equivalently, they are spatially Morita equivalent as enriched fusion categories [8,29]. Physically, it is because one can construct a gapless 0d domain walls between this gappable gapless edge and each of the two gapped edges. The physical reason is equivalent to the mathematical one. More details about this are given in [7,8].

Therefore, it is reasonable to ask if this gappable gapless edge describes the critical point of a purely edge topological phase transition between two gapped edges. The main goal of this work is to prove that this is indeed true. We will achieve this goal in Sec. IV by recovering the chiral symmetry V and all the ingredients of the enriched fusion category $(Z(\mathbf{Ising}),\ Z(\mathbf{Ising})_A)$, i.e., $M_{x,y}$, from a lattice model construction.

It is enough to just recover V and the partition function of $M_{x,y}$. In physics, the partition function of $M_{x,y}$ can be computed by the path integral over an annulus obtained by compactifying the time axis, and fixing the two boundary conditions to be x and y as shown in Fig. 4. The pictures in Fig. 4 also show that the partition function of $M_{x,y}$ is the same as that of $M_{\mathbb{1},x\star y}$. This is also obvious by the fact that $M_{x,y} = M_{\mathbb{1},x\star y}$ as objects in $Z(\mathbf{Ising})$. We denote the partition function of $M_{\mathbb{1},x} = x$ by $Z_x(\tau)$ for $x = \mathbb{1}, e, m, f, \chi_\pm$, where τ is the moduli of torus.

Since all $x = \mathbb{1}, e, m, f, \chi_\pm$ are obtained from double Ising topological order via an anyon condensation, they can all be viewed as objects in $\mathrm{Mod}_V \boxtimes \overline{\mathrm{Mod}_V}$ as shown in Eqs. (24) and

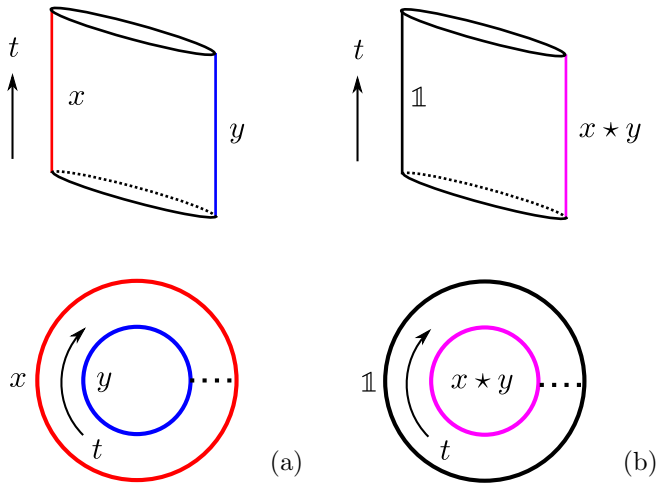

FIG. 4. Calculation of the partition function of $M_{x,y}$ via path integrals.

(25). Therefore, the partition function $Z_x(\tau)$ can be expressed in terms of the characters of $\mathbf{1}, \psi, \sigma$ in the Ising CFT, which are denoted by $\chi_0(\tau)$, $\chi_{\frac{1}{2}}(\tau)$, $\chi_{\frac{1}{16}}(\tau)$, respectively. Notice that 0, $\frac{1}{2}$, $\frac{1}{16}$ are the lowest conformal weights of $\mathbf{1}$, ψ, σ, respectively. By Eqs. (24) and (25), we obtain six partition functions $Z_x(\tau)$ for $x = \mathbb{1}, e, m, f, \chi_\pm$:

$$\chi_{\mathbb{1}}(\tau) = |\chi_0(\tau)|^2 + \left|\chi_{\frac{1}{2}}(\tau)\right|^2, \quad \chi_e = \chi_m = \left|\chi_{\frac{1}{16}}(\tau)\right|^2,$$
$$\chi_f = \chi_{\frac{1}{2}}(\tau)\chi_0(\tau)^* + \chi_0(\tau)\chi_{\frac{1}{2}}(\tau)^*, \tag{32}$$

$$\chi_{\chi_+}(\tau) = \chi_0(\tau)\chi_{\frac{1}{16}}(\tau)^* + \chi_{\frac{1}{2}}(\tau)\chi_{\frac{1}{16}}(\tau)^*,$$
$$\chi_{\chi_-}(\tau) = \chi_{\frac{1}{16}}(\tau)\chi_0(\tau)^* + \chi_{\frac{1}{16}}(\tau)\chi_{\frac{1}{2}}(\tau)^*. \tag{33}$$

We will show in Sec. IV explicitly how to recover these six partition functions $Z_x(\tau)$ (as summarized in Table I). The partition functions of $M_{x,y}$ are automatically recovered for exactly the same reason (as illustrated in Fig. 4), which is also manifest in the lattice model construction.

E. Second gappable gapless edge

In this section, we recall another gappable gapless edge of the 2d $\mathbb{Z}_2$ topological order [8]. This edge is closely related to the edge (30). Intrigued readers should consult [8] for more

TABLE I. Relation between the excitations in the bulk and the partition function of the CFT on the edge [recall Eqs. (32) and (33)].

	$(-)^\Phi$	$(-)^F$	Partition function
$\mathbb{1}$	$+1$	$+1$	$Z_{\mathbb{1}} = \lvert\chi_0(\tau)\rvert^2 + \lvert\chi_{\frac{1}{2}}(\tau)\rvert^2$
e	-1	$+1$	$Z_e = \lvert\chi_{\frac{1}{16}}(\tau)\rvert^2$
m	-1	-1	$Z_m = \lvert\chi_{\frac{1}{16}}(\tau)\rvert^2$
f	$+1$	-1	$Z_f = \chi_0(\tau)^*\chi_{\frac{1}{2}}(\tau) + \chi_{\frac{1}{2}}(\tau)^*\chi_0(\tau)$
χ_+	$+1$		$Z_{\chi_+} = \chi_{\frac{1}{16}}(\tau)^*\chi_0(\tau) + \chi_{\frac{1}{16}}(\tau)^*\chi_{\frac{1}{2}}(\tau)$
χ_-	-1		$Z_{\chi_-} = \chi_0(\tau)^*\chi_{\frac{1}{16}}(\tau) + \chi_{\frac{1}{2}}(\tau)^*\chi_{\frac{1}{16}}(\tau)$

gappable gapless edges of the 2d $\mathbb{Z}_2$ topological order. First, note that $V \otimes_{\mathbb{C}} \overline{V} \hookrightarrow A$, and A is a full field algebra extension of $V \otimes_{\mathbb{C}} \overline{V}$. Therefore, A can also be a nonchiral symmetry. There is a natural notion of Mod_A defined by the category of local A-module in $\mathrm{Mod}_V \boxtimes \overline{\mathrm{Mod}_V}$. In other words, Mod_A is again a UMTC and is equivalent to **Toric** containing four simple objects $\mathbb{1}, e, m, f$ as defined in (24).

Second, we enhance the nonchiral symmetry of the edge (30) from $V \otimes_{\mathbb{C}} \overline{V}$ to A. As a consequence, the simple edge excitations that preserve this enhanced nonchiral symmetry are reduced to $\mathbb{1}, e, m, f$ (see [8], Sec. 5.2)). We obtain a new gappable gapless edge defined by the following triple:

$$(A, \quad \mathrm{Mod}_A, \quad \textbf{Toric}). \tag{34}$$

The associated four partition functions are given in (32). If we insert the remaining two $\chi_\pm$ to the edge (34), it will break the nonchiral symmetry from A to $V \otimes_{\mathbb{C}} \overline{V}$. According to [8], this triple defines a new gappable gapless edge different from the one defined in (30). In this case, $M_{x,y}$ is the same as those in the edge (30) [recall (31)] except that x, y are restricted to only $\mathbb{1}, e, m, f$ and their direct sums. Therefore, there are only four relevant partition functions as listed in (32).

IV. A LATTICE MODEL REALIZATION

In this section, we give a lattice model realization of the critical point of the purely edge phase transition between two different gapped edges of the 2d $\mathbb{Z}_2$ topological order, and recover all the ingredients of the gappable gapless edge constructed in Sec. III C. We choose the Wen plaquette model to be the lattice realization of the 2d $\mathbb{Z}_2$ topological order. For the convenience of readers in mathematical background, we review the Wen plaquette model in details.

A. Wen plaquette model

The Wen plaquette model is defined on a square lattice with a two-dimensional local Hilbert space on each site, or one qubit per site. The Hamiltonian of this model is given by

$$H_{\mathrm{wp}} = -\sum_p O_p, \tag{35}$$

where p labels the plaquettes on the square lattice, as shown in Fig. 5(a). The operator O_p associated to the plaquette p acts on the four sites located at the four corners of the plaquette as

$$O_p = \overset{4}{\underset{1}{\square}}\!\!\overset{3}{\underset{2}{}} = \sigma_1^z\sigma_2^x\sigma_3^z\sigma_4^x. \tag{36}$$

where σ_i^x and σ_i^z are the qubit operators (represented as Pauli matrices) and the subscript i labels the site where these qubit operators are acting on. Here, we have adopted the diagrammatic representation introduced in [30], where each operator acting on a site is represented by a string going through that site, i.e., $\sigma_i^z \equiv$  and $\sigma_i^x \equiv$  . They anticommute with each other on the same site $\sigma_i^x\sigma_i^z = -\sigma_i^z\sigma_i^x$, which can be diagrammatically represented as (the operator

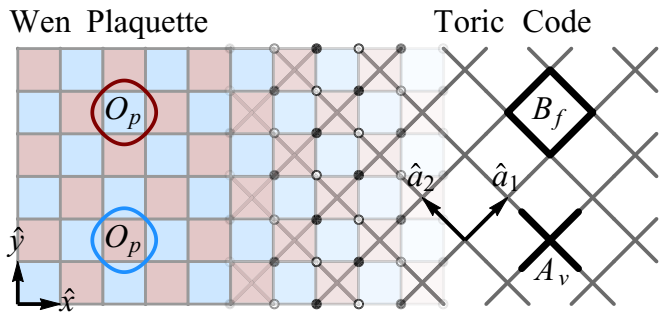

FIG. 5. Wen plaquette model on the square lattice (left) and its connection to the toric code model (right). The plaquette operator O_p maps to either the vertex operator A_v or the plaquette (face) operator B_f via local basis transformations of $\sigma^x \leftrightarrow \sigma^z$ on the hollow sites.

that acts later will be stacked above). In Fig. 5, the lattice is partitioned into red and blue plaquettes, but the operators O_p are defined identically for both types of plaquettes. This model $H_{\rm wp}$ is exactly solvable because for any pairs of plaquettes p and p', the operators O_p and $O_{p'}$ commute with each other, i.e.,

$$[O_p, O_{p'}] = 0. \tag{37}$$

Every state $|\mathrm{GS}\rangle$ in the ground-state Hilbert space of this model should satisfy

$$O_p|\mathrm{GS}\rangle = |\mathrm{GS}\rangle, \quad \forall\ \mathrm{p}. \tag{38}$$

So, O_p are also called the stabilizers that stabilize the ground state. In fact, every eigenstate of $H_{\rm wp}$ is a simultaneous eigenstate of O_p for all plaquettes p. By definition in Eq. (36), the eigenvalues of O_p are ± 1. Excited states of $H_{\rm wp}$ are labeled by a set of O_p eigenvalues containing -1. If an excited state carries a -1 eigenvalue of O_p for a given plaquette p, we say the excited state contains an excitation at the plaquette p.

The Wen plaquette model is in fact equivalent to the standard toric code model. To see this equivalence, we first reidentify the sites in the original square lattice (spanned by $\hat{x}, \hat{y}$) as the centers of the links in a new square lattice (spanned by $\hat{a}_1, \hat{a}_2$) which is 45° tilted from the original one as in shown in Fig. 5. A red plaquette of the original lattice will be associated to the sites in the new square lattice while a blue plaquette of the original lattice will be associated to the plaquette (face) of the new square lattice. We can transform the Wen plaquette model on the original lattice to the standard toric code model on the new tilted lattice. To do this, we perform a change of the basis on all the hollow sites (shown in Fig. 5) such that the role of σ^x and σ^z interchanges on those sites, i.e., $\sigma^x \leftrightarrow \sigma^z$. After this change of basis, the plaquette terms O_p on the blue plaquettes become the standard plaquette term $B_f = \prod_{l\in\partial f} \sigma_l^x$ of the toric code model on the orange lattice. In the new basis, the plaquette terms O_p on the red plaquettes become the standard vertex term $A_v = \prod_{l\in dv} \sigma_l^z$ of the toric code mode. The Hamiltonian in Eq. (35) then becomes $H = -\sum_v A_v - \sum_f B_f$ on the new lattice, which is the toric code model Hamiltonian.

In the toric code model, the A_v (or B_f) excitation is called the e (or m) particle. Following this convention, in the Wen plaquette model, the red (or blue) plaquette excitation should be labeled as e (or m) correspondingly. The bound state of e and m particles will be denoted as f, which is a fermion. These excitations can be created in pairs by string operators. The diagrammatic representation allows us to define string operators conveniently, simply by collecting the qubit operators along the string [see Fig. 6(a) for example]. Together with the trivial particle $\mathbb{1}$ (representing a local excitation), $\mathbb{1}, e, m, f$ form the set of simple objects in the toric code UMTC **Toric**.

Aside from these intrinsic excitations, the Wen plaquette model also admits extrinsic excitations such as lattice dislocations [4,31,32]. By an extrinsic excitation, we mean that the lattice dislocation is not an excited state in the spectrum of $H_{\rm wp}$ but rather a defect introduced to the system by modifying the Hamiltonian. The lattice dislocations are also created in pairs by removing a string of lattice sites, leaving two dislocation plaquettes at each end of the string, as shown in Fig. 6(b). The sites can be effectively removed by applying a strong external field to pin the qubits along the dislocation string, which amounts to adding the $H_{\rm dis} = g\sum_{i\in\text{string}} \sigma_i^x$ term to the Wen plaquette model $H_{\rm wp}$ [32]. The plaquette operator around the dislocation will be extended to the following five-qubit operator:

$$O_p = \mathrm{i}$$ 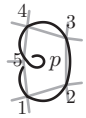 $$= -\sigma_1^z\sigma_2^x\sigma_3^z\sigma_4^x\sigma_5^y, \tag{39}$$

such that the local degeneracy around the dislocation can be lifted. The form of this dislocation plaquette operator can be derived from the $1/g$ perturbative expansion in the limit of strong pinning field $g \to \infty$ [32]. The introduction of the dislocation does not break the exact solvability of the model as the extended plaquette operator O_p (around the dislocation) still commutes with all the rest of the plaquette operators. So, all the eigenstates are still labeled by the eigenvalues of O_p operators. In particular, around a dislocation plaquette p, $O_p = +1$ stabilizes a trivial dislocation denoted as χ_+, while $O_p = -1$ indicates an excited dislocation denoted as χ_-. Both dislocation defects $\chi_\pm$ implement the e-m duality in the Wen plaquette model, as the lattice is distorted by the dislocation in such a way that there is no longer a global definition for red (e) and blue (m) plaquettes. If an e particle goes around one dislocation $\chi_\pm$, it will transmute into an m particle, and vice versa. Taking the dislocations $\chi_\pm$ into account, the six objects $\mathbb{1}, e, m, f, \chi_\pm$ are the simple objects in the UFC $Z(\mathbf{Ising})_A$ [recall Eqs. (24) and (25)]. The following fusion rules are evident by drawing diagrams of strings/dislocations:

$$\begin{aligned} e\star e = m\star m = f\star f = \mathbb{1}, \quad e\star m = f, \\ \chi_\pm\star\chi_\pm = \mathbb{1}\oplus f, \quad \chi_\pm\star\chi_\mp = e\oplus m, \\ e\star\chi_\pm = \chi_\pm\star e = m\star\chi_\pm = \chi_\pm\star m = \chi_\mp. \end{aligned} \tag{40}$$

For example, Figs. 6(b) and 6(c) show how χ_+ becomes χ_- by fusing with e or m (if we read the picture from left to right). They also illustrate $\chi_\pm\star\chi_\mp = e\oplus m$ (if we read the picture from top down or bottom up).

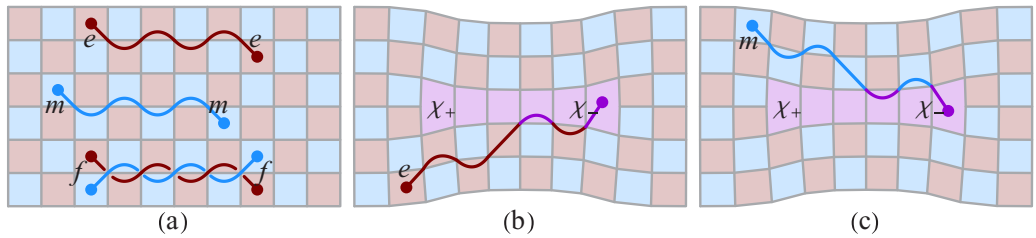

FIG. 6. (a) Intrinsic excitations are created in pairs by applying string operators to the ground state. Here, the red string operator creates a pair of e excitations, the blue string operator creates a pair of m excitations, and the intertwined red and blue strings create a pair of f excitations. (b), (c) Extrinsic excitations involve modifying the lattice. Here, we show a pair of dislocations: one plain dislocation χ_+ and one excited dislocation χ_-. χ_- can be obtained from χ_+ adding an excitation of either e or m (they are indistinguishable in the presence of dislocation).

B. Majorana representation

The Wen plaquette model also admits an alternative solution in terms of Majorana fermions. In this approach, the two-dimensional local Hilbert space $\mathbb{C}^2$ of a qubit on each site i is first lifted to a four-dimensional super vector space $\mathbb{C}^{2|2}$, equipped with four Majorana fermion operators $\gamma_i^0, \gamma_i^1, \gamma_i^2, \gamma_i^3$. The Majorana operators are Hermitian $\gamma_i^{a\dagger} = \gamma_i^a$ and satisfy the anticommutation relations $\{\gamma_i^a, \gamma_j^b\} = 2\delta_{ij}\delta^{ab}$. We then use the onsite projections $\mathbb{C}^{2|2} \to \mathbb{C}^2$ specified by $\gamma_i^0\gamma_i^1\gamma_i^2\gamma_i^3 = 1$ to restrict the fermion Hilbert space to the physical (qubit) Hilbert space, which corresponds to the even-fermion-parity sector on each site. This construction amounts to first fractionalize the qubit into Majorana fermions and then impose the projective constraint to remove the gauge redundancy introduced in the fractionalization procedure.

Under the constraint $\gamma_i^0\gamma_i^1\gamma_i^2\gamma_i^3 = 1$, each qubit operator σ_i^a $(a = x, y, z)$ can be represented as Majorana fermion bilinear operators in two seemingly different (but equivalent) ways:

$$\sigma_i^a = i\gamma_i^0\gamma_i^a = -i\epsilon^{abc}\gamma_i^b\gamma_i^c, \tag{41}$$

where a, b, c are used to label x, y, z or 1,2,3 interchangeably. It will be more intuitive to use the following diagrammatic representations:

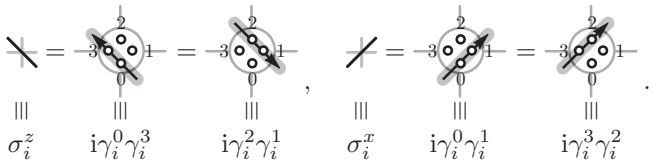

(42)

The four Majorana operators on each site are represented by small circles, and a string going through the site can pair up the fermion operators along the string in two different ways. The ordering of fermion operators is indicated by the arrow according to the following rules:

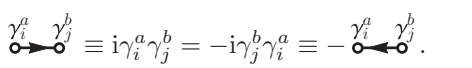

(43)

Using the Majorana representation, the plaquette operator O_p can be written as

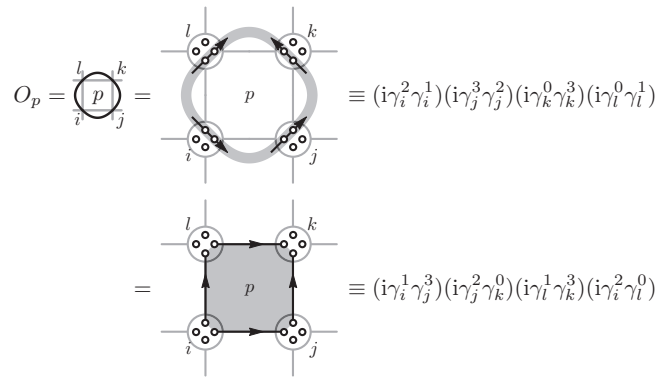

(44)

It will be convenient to introduce the link operators (as Majorana fermion bilinear terms across each link)

$$\hat{\tau}_{i,i+\hat{x}} = i\gamma_i^1\gamma_{i+\hat{x}}^3, \quad \hat{\tau}_{i,i+\hat{y}} = i\gamma_i^2\gamma_{i+\hat{y}}^0, \tag{45}$$

such that the plaquette operator $O_p = \prod_{\langle ij\rangle\in\partial p}\hat{\tau}_{ij}$ is simply a product of link operators around the plaquette. By definition, one can show that $\hat{\tau}_{ij}^\dagger = \hat{\tau}_{ij}$ and $\hat{\tau}_{ij}^2 = 1$, therefore, $\hat{\tau}_{ij}$ only have two possible eigenvalues $\tau_{ij} = \pm 1$. Moreover, the link operators $\hat{\tau}_{ij}$ commute with each other, so their eigenvalues τ_{ij} can be treated as independent $\mathbb{Z}_2$ variables. In the common eigenbasis of $\hat{\tau}_{ij}$, the Wen plaquette model is diagonalized $H_{\rm wp} = -\sum_p \prod_{\langle ij\rangle\in\partial p}\tau_{ij}$. If we identify the link variable τ_{ij} as a $\mathbb{Z}_2$ gauge connection along $\langle ij\rangle$, $H_{\rm wp}$ will describe a $\mathbb{Z}_2$ gauge theory, which is invariant under the gauge transformation $\tau_{ij} \to s_i\tau_{ij}s_j$ (induced by any configuration of $s_i = \pm 1$). The plaquette operator $O_p = \pm 1$ measures the $\mathbb{Z}_2$ gauge flux through each plaquette p ($O_p = 1$: no flux, $O_p = -1$: with flux). The Hamiltonian $H_{\rm wp} = -\sum_p O_p$ energetically favors the $\mathbb{Z}_2$ gauge flux to be trivial ($O_p = 1$) everywhere for the ground state.

Assuming periodic boundary conditions of the square lattice along both $\hat{x}$ and $\hat{y}$ directions, there will be four gauge-inequivalent configurations of τ_{ij} that solve the $O_p = 1$ constraints (see Fig. 7), which correspond to the four degenerated ground states of the Wen plaquette model on a torus. Each configuration of τ_{ij} specifies a unique fermion state $|\Psi[\tau_{ij}]\rangle$ in the fermion Hilbert space, s.t. $\hat{\tau}_{ij}|\Psi[\tau_{ij}]\rangle = \tau_{ij}|\Psi[\tau_{ij}]\rangle$, where all Majorana fermions are dimerized in pairs and fully gapped.

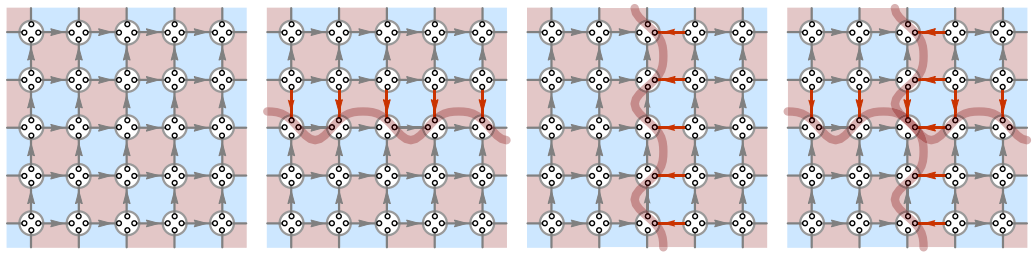

FIG. 7. Four gauge-inequivalent configurations of τ_{ij} that satisfy $O_p = 1$ for all plaquettes on a square lattice with periodic boundary condition in both directions. Link directions $i \to j$ to make $\tau_{ij} = +1$ are indicated by arrows, which point toward (against) $\hat{x}$ or $\hat{y}$ directions on the gray (red) links. These configurations are related to each other by applying string operators along noncontractible loops.

The physical ground state can be constructed by projection

$$|\mathrm{GS}\rangle = \prod_i \frac{1+\gamma_i^0\gamma_i^1\gamma_i^2\gamma_i^3}{2}|\Psi[\tau_{ij}]\rangle = \sum_{[s_i]}|\Psi[s_i\tau_{ij}s_j]\rangle. \quad (46)$$

Imposing the constraint $\gamma_i^0\gamma_i^1\gamma_i^2\gamma_i^3 = 1$ by projection is equivalent to summing over all gauge-related $|\Psi[s_i\tau_{ij}s_j]\rangle$ states (parametrized by $[s_i]$ that induces the gauge transform). Therefore, the four gauge-inequivalent sectors of the $O_p = 1$ subspace eventually result in the four physical ground states. The ground states are related to each other by string operators as shown in Fig. 7. In the Majorana representation, the string operator is proportional to the product of all Majorana operators covered by the string. Applying the string operator will change all $\gamma_i^a \to -\gamma_i^a$ along the string, and hence all $\tau_{ij} \to -\tau_{ij}$ if the link $\langle ij\rangle$ has an odd intersection with the string, thereby changing the state from one gauge sector to another.

C. Edge theory and partition functions

Now, we consider placing the Wen plaquette model on a square lattice with open boundaries. The Majorana fermions in the bulk still pair up and remain gapped, however, the dangling Majorana fermions along the edges of the system can become gapless. In general, any term that commutes with the plaquette terms O_p in the bulk can appear on the boundary, which will lift most of the edge degeneracy from the dangling Majorana modes and stabilize the edge theory. To the lowest order, the following edge terms will act on the links along the edge:

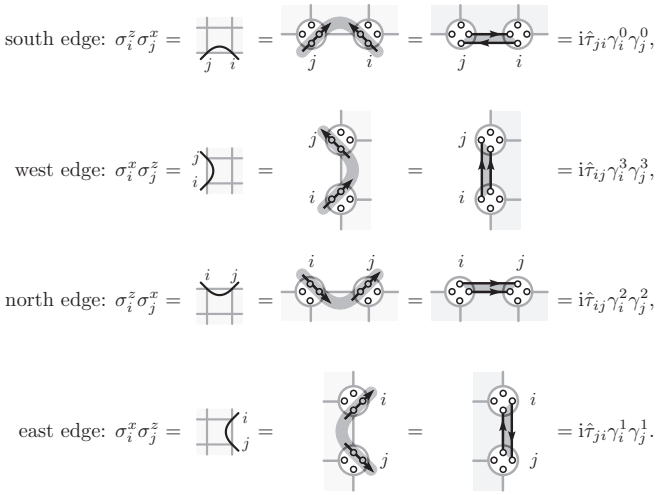

(47)

They describe the dangling Majorana fermions hopping on the edge and coupling to the gauge connection $\hat{\tau}_{ij} = -\hat{\tau}_{ji}$ on the edge link. Moreover, the four corner sites of the square lattice allows the following corner terms:

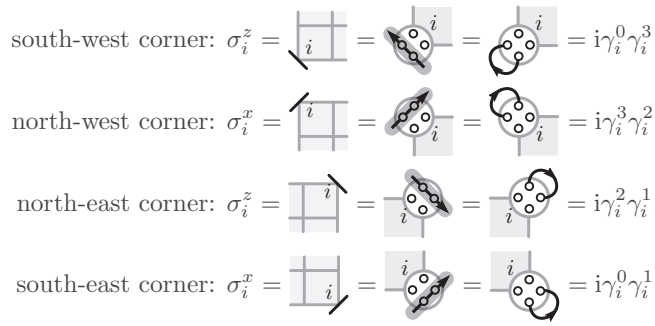

(48)

They describe how the Majorana fermion turns around at the corners. Gathering all these terms together and relabeling the dangling Majorana modes as ξ_i (see Fig. 8), the boundary of Wen plaquette model realizes a closed Majorana chain coupled to a $\mathbb{Z}_2$ gauge field (originated from the bulk), which

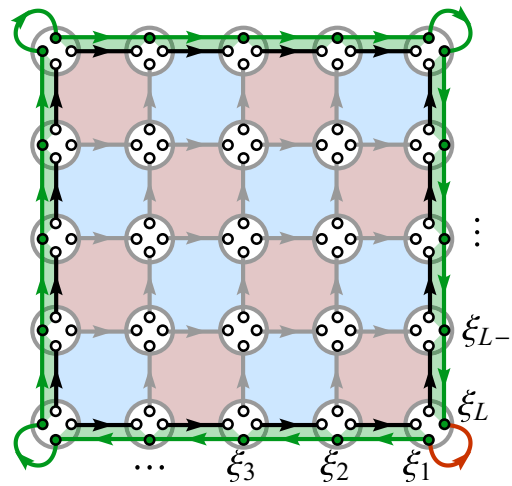

FIG. 8. The Majorana representation of the Wen plaquette model with open boundary. The dangling Majorana modes along the edge are marked as green dots. They are connected by the edge terms to form a Majorana chain coupled to the $\mathbb{Z}_2$ gauge theory in the bulk. The red plaquettes are even (e) plaquettes and the blue plaquettes are odd (m) plaquettes.

is described by the following edge Hamiltonian:

$$H_{\text{bdy}} = -\sum_{i=1}^{L-1} it_{i,i+1}\xi_i\xi_{i+1} - it_{L,1}\xi_L\xi_1, \tag{49}$$

where the total number of Majorana modes is $L = 2(L_x + L_y)$ on a $L_x \times L_y$ lattice. The gauge connection t_{ij} in H_{bdy} is tied to the gauge connection τ_{ij} along the edge link according to Eq. (47) as

$$t_{ij} = \begin{cases} \tau_{ij} & \langle ij\rangle \text{ on the west and north edges,} \\ \tau_{ji} = -\tau_{ij} & \langle ij\rangle \text{ on the east and south edges.} \end{cases} \tag{50}$$

For the corners, t_{ij} are fixed by Eq. (48) to be $t_{L1} = -1$ on the southeast corner and $t_{i,i+1} = +1$ on the rest of the corners (as illustrated in Fig. 8).

First of all, the edge is gapless. For any configuration of the gauge field t_{ij}, we can show that there always exist gauge-invariant excitations in the spectrum of H_{bdy} whose excitation energy ΔE lies below $4\pi/L$. Because along the one-dimensional edge, we can always gauge away the nontrivial gauge connection to the boundary condition, i.e., any configuration of t_{ij} can be related to $t_{i,i+1} = 1$ ($i = 1, 2, \ldots, L-1$) and $t_{L1} = \pm 1$ by gauge transformation. Then, Fourier transforming to the momentum space $\xi_k = L^{-1/2}\sum_{i=1}^{L}\xi_i e^{-iki}$, the boundary Hamiltonian in Eq. (49) can be diagonalized as $H_{\text{bdy}} = \sum_{0<k<\pi}\epsilon_k\xi_{-k}\xi_k$, where $\epsilon_k = 2\sin k$ describes the single-particle excitation energy ϵ_k as a function of the momentum k. Note that for Majorana fermions $\xi_{-k} = \xi_k^\dagger$, so ξ_k at $k = 0, \pi$ (if realizable) are Majorana operators (zero modes) and ξ_k with $0 < k < \pi$ are annihilation operators of fermion excitations. The excitation spectrum of H_{bdy} can be labeled by fermion occupation numbers $n_k = \xi_{-k}\xi_k = 0, 1$ (for $0 < k < \pi$) subject to the condition that the fermions can only be excited in pairs to maintain gauge invariance. Consider two-fermion excitations, the excitation energies are given by $\Delta E_{(k_1,k_2)} = \epsilon_{k_1} + \epsilon_{k_2}$ and labeled by two momenta k_1 and k_2. The boundary condition $t_{L1} = \pm 1$ only affects the momentum quantization between $k = 2\pi n/L$ (for $n = 0, \ldots, L/2$) or $k = 2\pi(n + 1/2)/L$ (for $n = 0, \ldots, L/2 - 1$). For $t_{L1} = +1$ (or $t_{L1} = -1$), we can explicitly construct the gauge-invariant excitation of $\Delta E_{(0,2\pi/L)} = 2\sin 2\pi/L$ (or $\Delta E_{(\pi/L,\pi/L)} = 4\sin\pi/L$). In either case, the minimal excitation energy is bounded by $\Delta E \leqslant 4\pi/L$ at least. So, the edge excitations gap vanishes (as $\sim 1/L$) in the $L \to \infty$ thermodynamic limit.

Moreover, the edge is anomalous, in correspondence to the $\mathbb{Z}_2$ topological order in the bulk. This is manifest from the fact that the edge Hamiltonian H_{bdy} in Eq. (49) is not a standalone one-dimensional model but has to involve the $\mathbb{Z}_2$ gauge field from the bulk. To further expose the edge anomaly, we study how the edge partition function responses to different bulk excitations (including both intrinsic and extrinsic excitations). This in turn establishes a bulk-edge correspondence between the $\mathbb{Z}_2$ topological order **Toric** in the bulk and its gapless edge.

The same conclusion can be obtained on the field-theory level [11] by connecting the mutual Chern-Simons theory description of the bulk $\mathbb{Z}_2$ topological order to the Luttinger-liquid description of the edge Ising criticality. The result is also supported by the analysis of effective edge Hamiltonian based on the tensor network representation of $\mathbb{Z}_2$ topological ordered state [33]. Here, we provide a lattice derivation of the bulk-edge correspondence based on the Majorana representation, which enables us to further discuss the effect of bulk excitations (especially extrinsic excitations) on the edge theory.

We start from intrinsic excitations $\mathbb{1}, e, m, f$. To facilitate our discussion, we define the total $\mathbb{Z}_2$ flux operator $(-)^\Phi$ and the edge fermion parity operator $(-)^F$ as

$$(-)^\Phi = -t_{L1}\prod_{i=1}^{L-1} t_{i,i+1}, \quad (-)^F = \prod_{r=1}^{L/2} it_{2r-1,2r}\xi_{2r-1}\xi_{2r}. \tag{51}$$

Both of them are invariant under gauge transformations $\xi_i \to s_i\xi_i$ and $t_{ij} \to s_i t_{ij} s_j$ (for any $s_i = \pm 1$). To make their physical meaning more explicit, we can use the gauge freedom to fix $t_{i,i+1} = 1$ for $i = 1, 2, \ldots, L-1$ and push all the nontrivial gauge connection to the boundary condition $t_{L1} = \pm 1$. After gauge fixing, $(-)^\Phi = -t_{L1}$ measures the total $\mathbb{Z}_2$ gauge flux enclosed by the Majorana chain, such that $(-)^\Phi = 1$ [or $(-)^\Phi = -1$] corresponds to the no-flux (or π-flux) case, which also corresponds to the Neveu-Schwarz (or Ramond) boundary condition for the Majorana fermion ξ_i. Also, with this gauge choice, $(-)^F = \prod_{r=1}^{L/2} i\xi_{2r-1}\xi_{2r}$ becomes the product of all dangling Majorana fermions ξ_i, which matches the definition of fermion parity in a purely one-dimensional Majorana chain. In conclusion, Eq. (51) provides a gauge-independent definition of the $\mathbb{Z}_2$ flux $(-)^\Phi$ and edge fermion parity $(-)^F$ operators, which allows us to make connection to the plaquette operators in the bulk. Using the relation between t_{ij} and τ_{ij} in Eq. (50) and using the fact that the total fermion parity of the system is even, it can be shown that

$$(-)^\Phi = \prod_p O_p, \quad (-)^F = \prod_{p\in\text{odd}} O_p. \tag{52}$$

The even and odd plaquettes are assigned such that the plaquette on the southeast corner (the corner of ξ_1 and ξ_L) is always defined to be even, and the rest of the plaquettes can be labeled odd or even following the checkerboard pattern (see Fig. 8). We will follow the convention to call the excitation in the even (odd) plaquette as the e (m) excitation, and treat f as the bound state of e and m. Then, according to Eq. (52), $(-)^\Phi$ counts the parity of e and m particles and $(-)^F$ counts the parity of m and f particles in the bulk. Therefore, pushing the bulk particle to the edge can change the $\mathbb{Z}_2$ flux and fermion parity of the Majorana chain, which is reflected in the change of the partition function of the edge theory. The results are summarized in Table I and will be explained later in details.

To calculate these partition functions, we work with the $t_{i,i+1} = 1$ gauge (for $i = 1, 2, \ldots, L-1$). The Majorana chain can be described by a free-fermion CFT at low energy. As we discussed, the edge fermion dispersion relation is given by $\epsilon_k = 2\sin k$. Hence, the low-energy fermions are described by the fermion modes with momenta $k = 0 + k_L$ and $k = \pi + k_R$ for small k_L and k_R. As we will see, the fermion modes with small k_L and k_R correspond to the left-moving and right-moving fermion modes in terms of the (1+1)D free-fermion CFT. By linearizing the dispersion for small k_L and k_R, we can write the Hamiltonian H and the total momentum P in the

momentum space:

$$H = \sum_{k_L} v_F k_L n_{k_L} + \sum_{k_R} -v_F k_R n_{k_R},$$
$$P = \sum_{k_L} k_L n_{k_L} + \sum_{k_R} k_R n_{k_R}, \tag{53}$$

where the Fermi velocity happens to be $v_F = 2$ for the lattice model in Eq. (49). $n_{k_L} = 0, 1$ and $n_{k_R} = 0, 1$ denote the fermion occupation number of the momentum $k = 0 + k_L$ and $k = \pi + k_R$ modes. We notice that both the Hamiltonian H and the total momentum P receive contributions separately from the left- and right-moving fermion modes.

Without a $\mathbb{Z}_2$ flux in the bulk $(-)^\Phi = -t_{L1} = +1$, the fermion sees an antiperiodic boundary condition (as $t_{L1} = -1$) on the lattice and and its momentum is quantized to $k = 2\pi(n + 1/2)/L$ (for $n \in \mathbb{Z}$). Since L is even, the quantization of k_L and k_R is consequently given by $k_L = 2\pi(n' + 1/2)/L$ and $k_R = 2\pi(n'' + 1/2)/L$ with $n', n'' \in \mathbb{Z}$. This quantization of k_L and k_R implies that the left- and right-moving fermions are both subject to the Neveu-Schwarz (NS) boundary condition, namely, the antiperiodic boundary condition in the CFT sense, in the spatial direction. Here, the boundary conditions for the left- and right-moving fermion modes are the same and are identical to the boundary condition defined on the lattice. However, one always needs to be cautious that these boundary conditions are not necessarily equal. We will encounter such cases in the presence of the dislocations $\chi_\pm$.

The partition function on a space-time torus with modular parameter $\tau = (\alpha + i\beta v_F)/L$ for both even and odd fermion parity will be given by

$$Z_{\mathbb{1}}(\tau) = \mathrm{Tr}_{\mathrm{NS}} \frac{1 + (-)^F}{2} e^{-\beta H + i\alpha P},$$
$$Z_f(\tau) = \mathrm{Tr}_{\mathrm{NS}} \frac{1 - (-)^F}{2} e^{-\beta H + i\alpha P}, \tag{54}$$

where $\mathrm{Tr}_{\mathrm{NS}}$ represents the trace over the left- and right-moving fermion modes with the k_L and k_R quantization discussed above. These partition functions can be calculated by calculating the two terms $\mathrm{Tr}_{\mathrm{NS}} e^{-\beta H + i\alpha P}$ and $\mathrm{Tr}_{\mathrm{NS}} (-)^F e^{-\beta H + i\alpha P}$ separately. The form of the Hamiltonian H and the total momentum P given in Eq. (53), together with the fact that the total fermion parity operator $(-)^F$ is a product of the left- and right-fermion parities, ensures that each of $\mathrm{Tr}_{\mathrm{NS}} e^{-\beta H + i\alpha P}$ and $\mathrm{Tr}_{\mathrm{NS}} (-)^F e^{-\beta H + i\alpha P}$ factorizes into a product of the left-moving-fermion contribution and the right-moving-fermion contribution:

$$\mathrm{Tr}_{\mathrm{NS}}\, e^{-\beta H + i\alpha P} = |d_{--}(\tau)|^2,$$
$$\mathrm{Tr}_{\mathrm{NS}}\, (-)^F e^{-\beta H + i\alpha P} = |d_{-+}(\tau)|^2, \tag{55}$$

where $d_{-\mp}(\tau) = q^{-\frac{1}{48}} \prod_{n=0}^{\infty} (1 \pm q^{n+1/2})$ with $q = e^{2\pi i \tau}$ are the contributions from the left-moving fermions. The contributions from the right-moving fermions are given by $d_{-\mp}(\tau)^*$. Details of $d_{-\mp}(\tau)$ can be found in Chapter 6.4 and Chapter 10.3 in [34]. The two subscripts of $d_{-\pm}(\tau)$ represent the spatial and temporal boundary conditions (in the CFT sense) respectively: "−" represents the antiperiodic (Neveu-Schwarz) boundary condition and "+" represents the periodic (Ramond) boundary condition. Here, the trace $\mathrm{Tr}_{\mathrm{NS}}$ has already set the spatial boundary condition for both of the left- and right-moving modes to be antiperiodic (Neveu-Schwarz). The temporal boundary condition is periodic (Ramond) if there is a fermion parity operator $(-)^F$ in the trace $\mathrm{Tr}_{\mathrm{NS}}$. It is antiperiodic (Neveu-Schwarz) if without. Putting the results together, we have

$$Z_{\mathbb{1}}(\tau) = \mathrm{Tr}_{\mathrm{NS}} \frac{1 + (-)^F}{2} e^{-\beta H + i\alpha P} = \frac{|d_{--}(\tau)|^2 + |d_{-+}(\tau)|^2}{2},$$
$$Z_f(\tau) = \mathrm{Tr}_{\mathrm{NS}} \frac{1 - (-)^F}{2} e^{-\beta H + i\alpha P} = \frac{|d_{--}(\tau)|^2 - |d_{-+}(\tau)|^2}{2}. \tag{56}$$

With a $\mathbb{Z}_2$ flux in the bulk $(-)^\Phi = -t_{L1} = -1$, the fermion sees a periodic boundary condition (as $t_{L1} = +1$) on the lattice and its momentum is quantized to $k = 2\pi n/L$ (for $n \in \mathbb{Z}$). Given that L is even, the momenta of left- and right-moving fermion modes are then correspondingly quantized to $k_L = 2\pi n'/L$ and $k_R = 2\pi n''/L$ with $n', n'' \in \mathbb{Z}$. This quantization of k_L and k_R implies that the left- and right-moving fermions are both subject to the Ramond (R) boundary condition, namely, the periodic boundary condition in the CFT sense, in the spatial direction. Notice that this spatial periodic boundary condition allows for fermion zero modes at $k_L = 0$ and at $k_R = 0$. In this case, the partition function in both fermion parity sectors will be given by

$$Z_e(\tau) = \mathrm{Tr}_{\mathrm{R}} \frac{1 + (-)^F}{2} e^{-\beta H + i\alpha P} = \frac{|d_{+-}(\tau)|^2 + |d_{++}(\tau)|^2}{2},$$
$$Z_m(\tau) = \mathrm{Tr}_{\mathrm{R}} \frac{1 - (-)^F}{2} e^{-\beta H + i\alpha P} = \frac{|d_{+-}(\tau)|^2 - |d_{++}(\tau)|^2}{2}, \tag{57}$$

where $d_{+\mp}(\tau) = \frac{1}{\sqrt{2}} q^{\frac{1}{24}} \prod_{n=0}^{\infty} (1 \pm q^n)$ with $q = e^{2\pi i \tau}$. Here, Tr_{R} represents the trace over the left- and right-moving fermion modes with the k_L and k_R quantization given above. The $\frac{1}{\sqrt{2}}$ factor takes care of the state counting in the presence of the zero mode. Here, the two subscripts of $d_{+\mp}(\tau)$ again labels the spatial and temporal boundary conditions, respectively. These results are obtained in a similar fashion as $Z_{\mathbb{1}}(\tau)$ and $Z_f(\tau)$. Details of $d_{+\mp}(\tau)$ can also be found in Chap.s 6.4 and 10.3 in [34]. Interestingly, we notice that $d_{++}(\tau) = 0$ due to the $n = 0$ contributions. Hence,

$$Z_e(\tau) = Z_m(\tau). \tag{58}$$

The characters $d_{\pm\pm}(\tau)$ are in fact the partitions of the (1+1)D free-fermion CFT on the torus with different boundary conditions (or equivalently different spin structures). It is a classic result that the free-fermion characters $d_{\pm\pm}(\tau)$ can be directly related to the characters χ_0, $\chi_{\frac{1}{16}}$, $\chi_{\frac{1}{2}}$ of the Ising CFT (see, for instance, Chap. 10.3 of [34] for reference) in the following way:

$$\chi_0(\tau) = \frac{d_{--}(\tau) + d_{-+}(\tau)}{2},$$
$$\chi_{\frac{1}{16}}(\tau) = \frac{d_{+-}(\tau)}{\sqrt{2}},$$
$$\chi_{\frac{1}{2}}(\tau) = \frac{d_{--}(\tau) - d_{-+}(\tau)}{2}. \tag{59}$$

Therefore, we can rewrite the partition functions $Z_{\mathbb{1}}$, $Z_e(\tau)$, $Z_m(\tau)$, and $Z_f(\tau)$ as

$$\begin{aligned} Z_{\mathbb{1}} &= |\chi_0(\tau)|^2 + \left|\chi_{\frac{1}{2}}(\tau)\right|^2, \\ Z_f &= \chi_0(\tau)^* \chi_{\frac{1}{2}}(\tau) + \chi_{\frac{1}{2}}(\tau)^* \chi_0(\tau), \\ Z_e(\tau) &= Z_m(\tau) = \left|\chi_{\frac{1}{16}}(\tau)\right|^2. \end{aligned} \tag{60}$$

In this way, we have provided an explicit lattice model realization of all partition functions [recall Eq. (32)] on the gappable nonchiral gapless edges defined in (34). If we impose the nonchiral symmetry A [recall (18)] at the critical point, these are the only partition functions preserving the nonchiral symmetry A (see ([8], Sec. 5.2)).

In fact, some more interpretation of the partition functions is in order. In defining $Z_{\mathbb{1}}$, $Z_e(\tau)$, $Z_m(\tau)$, and $Z_f(\tau)$, we only consider the low-energy edge degrees of freedom in the traces "$\mathrm{Tr}_{\mathrm{NS}}$" and "$\mathrm{Tr}_{\mathrm{R}}$." However, these partition functions can still be interpreted as the partition functions for whole system (including the edge and the bulk degrees of freedom) with the bulk in the "infinite-gap limit." The bulk energy gap is set by the energy scale of the bulk Hamiltonian H_{wp} while the edge energy scale is set independently by H_{bdy}. For a finite-size system, if we take the bulk energy gap to be infinite without changing the edge energy scale, the whole system will be automatically in the sector with $(-)^{\Phi} = (-)^F = 1$ at low energy. The partition function of the whole system then receives contributions only from the gapless edge states in the corresponding sector and becomes $Z_{\mathbb{1}}(\tau)$ in this limit. To obtain $Z_m(\tau)$ as the partition function of the whole system, we need to change the bulk Hamiltonian H_{wp} on a single odd plaquette p. By changing the sign of the coupling for the operator O_p on the given (odd) plaquette p, we obtain a new Hamiltonian H'_{wp} whose infinite-gap limit automatically favors the sector with $(-)^{\Phi} = -1$ and $(-)^F = -1$ at low energy. In this limit, the partition function of the whole system receives contributions only from the gapless edge states in the corresponding sector and becomes $Z_m(\tau)$. $Z_e(\tau)$ and $Z_f(\tau)$ can be obtained in a similar way as the partition functions of the whole system.

In the following, we discuss the behavior of these partition functions $Z_{\mathbb{1}}(\tau)$, $Z_f(\tau)$, $Z_e(\tau)$, and $Z_m(\tau)$ under modular transformations. The characters $d_{\pm\pm}(\tau)$ have simple modular transformation properties:

$$\mathcal{S} \text{ transformation } \tau \to -1/\tau : \begin{cases} d_{++}(-1/\tau) = d_{++}(\tau) = 0, \\ d_{+-}(-1/\tau) = d_{-+}(\tau), \\ d_{-+}(-1/\tau) = d_{+-}(\tau), \\ d_{--}(-1/\tau) = d_{--}(\tau), \end{cases} \tag{61}$$

$$\mathcal{T} \text{ transformation } \tau \to \tau + 1 : \begin{cases} d_{++}(\tau+1) = d_{++}(\tau) = 0, \\ d_{+-}(\tau+1) = e^{i2\pi/24} d_{+-}(\tau), \\ d_{-+}(\tau+1) = e^{-i2\pi/48} d_{--}(\tau), \\ d_{--}(\tau+1) = e^{-i2\pi/48} d_{-+}(\tau). \end{cases} \tag{62}$$

These transformations induce the modular transformations of $Z_{\mathbb{1}}(\tau)$, $Z_f(\tau)$, $Z_e(\tau)$, and $Z_m(\tau)$:

$$\begin{pmatrix} Z_{\mathbb{1}}(-1/\tau) \\ Z_e(-1/\tau) \\ Z_m(-1/\tau) \\ Z_f(-1/\tau) \end{pmatrix} = S \begin{pmatrix} Z_{\mathbb{1}}(\tau) \\ Z_e(\tau) \\ Z_m(\tau) \\ Z_f(\tau) \end{pmatrix}, \quad \begin{pmatrix} Z_{\mathbb{1}}(\tau+1) \\ Z_e(\tau+1) \\ Z_m(\tau+1) \\ Z_f(\tau+1) \end{pmatrix} = T \begin{pmatrix} Z_{\mathbb{1}}(\tau) \\ Z_e(\tau) \\ Z_m(\tau) \\ Z_f(\tau) \end{pmatrix}, \tag{63}$$

where the matrices S and T are given by

$$S = \frac{1}{2} \begin{pmatrix} 1 & 1 & 1 & 1 \\ 1 & 1 & -1 & -1 \\ 1 & -1 & 1 & -1 \\ 1 & -1 & -1 & 1 \end{pmatrix}, \quad T = \begin{pmatrix} 1 & 0 & 0 & 0 \\ 0 & 1 & 0 & 0 \\ 0 & 0 & 1 & 0 \\ 0 & 0 & 0 & -1 \end{pmatrix}. \tag{64}$$

In fact, Eq. (63) does NOT uniquely determine S and T. However, the S and T matrices given above match exactly the modular S and T matrices of the $\mathbb{Z}_2$ topological order. This is not surprising because of Eq. (24). That the partition functions on the gapless edge transform covariantly according to the S and T matrices associated to the bulk 2d phase is true for all the so-called canonical chiral or nonchiral gapless edges almost tautologically according to the general theory in ([7,8], Theorem$^{\mathrm{ph}}$ 5.16).[2]

Another observation is that $Z_{\mathbb{1}} + Z_m$ (or $Z_{\mathbb{1}} + Z_e$) matches exactly the Ising CFT partition function on a torus which is modular invariant. This is not surprising because of (24).

If we are allowed to break the nonchiral symmetry from A to $\mathbf{1} \boxtimes \mathbf{1} = V \otimes_{\mathbb{C}} \overline{V} \subset A$ [recall (18)] at the critical point by adding the extrinsic excitations $\chi_{\pm}$ (see ([8], Sec. 5.2)), we can obtain a lattice realization of the gapless edge defined by $(V \otimes_{\mathbb{C}} \overline{V}, Z(\mathbf{Ising}), Z(\mathbf{Ising})_A)$ [recall Eq. (30)]. The extrinsic excitations $\chi_{\pm}$ correspond to lattice dislocations in the bulk. If we create a pair of lattice dislocations and push one of them through the edge, the number of lattice sites along the edge will be effectively reduced by one, resulting in an odd number of dangling fermions on the edge, as shown

[2] Ji and Wen amplified this fact in [35] and promoted it to a general principle even in higher dimensions. For general chiral or nonchiral gapless edges, this statement is true in many cases. But, there are counterexamples (see ([8], Example 5.17)). We believe that this fact can be generalized even to higher dimensions but under certain unknown conditions.

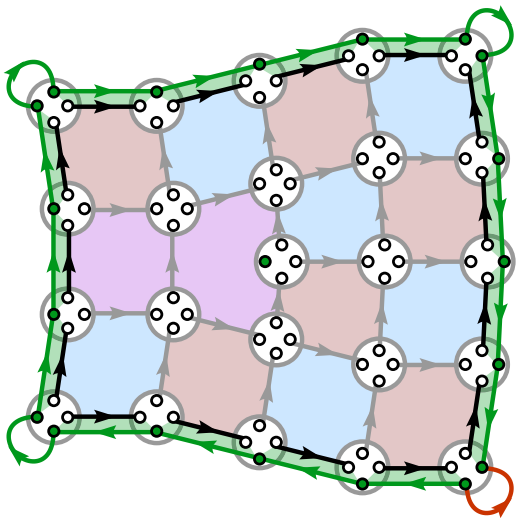

FIG. 9. The Majorana representation of the Wen plaquette model in the presence of a dislocation χ_+. Green dots mark out the dangling Majorana modes along the edge as well as the Majorana zero mode trapped by the dislocation inside the bulk. The number of Majorana modes on the edge becomes odd. The even(e)/odd(m) plaquette can no longer be globally defined (the inconsistent plaquettes are colored in purple).

in Fig. 9. To compensate the missing Majorana mode on the edge, one Majorana zero mode will appear at the dislocation inside the bulk. In this case, the edge fermion parity operator can no longer be defined (as there are only an odd number of fermion modes on the edge). This is also manifest from the bulk that the plaquettes can not be consistently assigned as even/odd in the presence of the dislocation. Therefore, $(-)^F$ in Eq. (52) no longer makes sense. Nevertheless, the total $\mathbb{Z}_2$ flux $(-)^\Phi$ is still well defined as $(-)^\Phi = -t_{L1}\prod_{i=1}^{L-1} t_{i,i+1} = \prod_p O_p$ as long as the plaquette operator is extended around the dislocation according to Eq. (39). Therefore, in the absence of excitations in the regular (nondislocation) plaquettes, the trivial χ_+ and excited χ_- dislocations in the bulk will lead to different boundary conditions for the boundary Majorana chain. Namely, $(-)^\Phi = \pm 1$ corresponds to $\chi_\pm$.

Interestingly, the presence of a single dislocation in the bulk renders the length L of the edge Majorana chain odd. In this case, the boundary condition defined on the lattice for the edge Majorana chain is translated in the nontrivial way into the boundary condition (in the CFT sense) for the left- and right-moving fermion modes. Let us start with the dislocation χ_+ which leads to $(-)^\Phi = +1$. The edge fermion modes experience an antiperiodic boundary condition on the lattice. Hence, their momenta are quantized to $k = 2\pi(n+1/2)/L$ with $n \in \mathbb{Z}$. At low energy, we focus on the left- and right-moving fermion modes with momenta $k = 0 + k_L$ and $k_R = \pi + k_R$. When L is odd, the quantization $k = 2\pi(n+1/2)/L$ leads to the quantization $k_L = 2\pi(n'+1/2)/L$ and $k_R = 2\pi n''/L$ with $n', n'' \in \mathbb{Z}$ for the left- and right-moving fermions. We notice that k_L and k_R are now quantized differently. These quantizations suggest that the left-moving fermion modes are subject to an antiperiodic (Neveu-Schwarz) boundary condition in a CFT sense, while the right-moving fermions are subject to a periodic (Ramond) boundary condition in a CFT sense. Therefore, the partition function is given by

$$Z_{\chi_+}(\tau) = \frac{1}{\sqrt{2}} d_{+-}(\tau)^* d_{--}(\tau), \tag{65}$$

where $d_{--}(\tau)$ and $d_{+-}(\tau)^*$ are the contributions from the left- and right-moving fermions. They are both subject to an antiperiodic boundary condition in the temporal direction. That is because there is no edge fermion parity projection needed and, hence, no edge fermion parity operator involved in obtaining $Z_{\chi_+}(\tau)$. $d_{--}(\tau)$ and $d_{+-}(\tau)^*$ have the opposite spatial boundary conditions because the momentum quantization of k_L and k_R explained above. The reason that there is an extra factor of $\frac{1}{\sqrt{2}}$ in $Z_{\chi_+}(\tau)$ is a bit tricky. First of all, the edge Majorana chain with an odd length does not, strictly speaking, have a well-defined Hilbert space. One natural solution to it is to consider the total Hilbert space defined by both the edge fermion modes and the Majorana zero mode localized on the dislocation (even though the latter is decoupled from the former). This Majorana zero mode on the dislocation should contribute a $\sqrt{2}$ factor based on its quantum dimension. However, we need to ensure that the global fermion parity (including the edge and dislocation Majorana modes) is even (so that the states involved in the partition sum can be projected back to the "bosonic" Hilbert space with just bosonic spin operators acting on it). The global fermion parity projection eliminates half of the states in the fermionic Hilbert space (associated to the Majorana modes) and hence leads to an extra factor of $\frac{1}{2}$. Therefore, the quantum dimension of the dislocation Majorana zero mode and the global fermion parity projection in total contribute to a factor of $\frac{\sqrt{2}}{2}$ to the partition function. Including the Majorana zero mode on the dislocation and implementing the global fermion parity projection are also natural if we consider $Z_{\chi_+}(\tau)$ as the partition function of the whole system (including the bulk and the edge) in the infinite-gap limit. That is because the Majorana zero mode localized on the dislocation has zero energy even when the bulk is in the infinite-gap limit. Furthermore, the global fermion parity projection is always needed to ensure the states summed over in the partition function live in a bosonic Hilbert space.

We can analyze the case with a χ_- dislocation in a similar way. The dislocation χ_- which leads to $(-)^\Phi = -1$. Hence, the edge fermion modes experience a periodic boundary condition on the lattice. Their momenta are therefore quantized to $k = 2\pi n/L$ with $n \in \mathbb{Z}$. At low energy, we focus on the left- and right-moving fermion modes with momenta $k = 0 + k_L$ and $k_R = \pi + k_R$. When L is odd, the quantization $k = 2\pi n/L$ leads to the quantization $k_L = 2\pi n'/L$ and $k_R = 2\pi(n''+1/2)/L$ with $n', n'' \in \mathbb{Z}$ for the left- and right-moving fermions. Again, k_L and k_R are quantized differently. In the CFT sense, the left-moving fermion modes are now subject to a periodic (Ramond) boundary condition, while the right-moving fermions are subject to an antiperiodic (Neveu-Schwarz) boundary condition. Therefore, the partition function is given by

$$Z_{\chi_-}(\tau) = \frac{1}{\sqrt{2}} d_{--}(\tau)^* d_{+-}(\tau). \tag{66}$$

In terms of the Ising CFT characters, we can write

$$Z_{\chi_+}(\tau) = \chi_{\frac{1}{16}}(\tau)^* \chi_0(\tau) + \chi_{\frac{1}{16}}(\tau)^* \chi_{\frac{1}{2}}(\tau),$$
$$Z_{\chi_-}(\tau) = \chi_0(\tau)^* \chi_{\frac{1}{16}}(\tau) + \chi_{\frac{1}{2}}(\tau)^* \chi_{\frac{1}{16}}(\tau). \quad (67)$$

We see immediately that we have achieved the lattice model realization of the last two partition functions (33) in the enriched fusion category of the gapless edge defined by the triple $(V \otimes_{\mathbb{C}} \overline{V},\ Z(\textbf{Ising}),\ Z(\textbf{Ising})_A)$ [recall Eq. (30)]. All the partition functions $Z_{\mathbb{1}}$, Z_e, Z_m, Z_f, Z_{χ_+}, and Z_{χ_-} are summarized in Table I.

We have recovered the partition functions of $M_{\mathbb{1},x}$ for $x = \mathbb{1}, e, m, f, \chi_\pm$ on the edge (30) directly from the lattice model of the gapless edge. More general partition function of $M_{x,y}$ coincides with that of $M_{\mathbb{1},x\otimes y}$. This is obvious from our lattice model construction. Therefore, the gapless edge defined by Eq. (49), which is coupled to the bulk, realizes physically the gapless edge defined by the triple $(V \otimes_{\mathbb{C}} \overline{V}, Z(\textbf{Ising}), Z(\textbf{Ising})_A)$.

The partition functions $Z_{\mathbb{1}}, Z_e, Z_m, Z_f, Z_{\chi_+}$ obtained using a Hamiltonian formalism in this section are closely related to the results of [36] where the Ising CFT partition functions in the presence of topological line defects are studied using a two-dimensional statistical mechanical model. The two-dimensional statistical mechanical model proposed in [36] can be viewed as the discretized Euclidean path integral of the edge Hamiltonian studied in this section. The topological defect lines of the statistical mechanical can be identified as the world line of the objects $x = \mathbb{1}, e, m, f, \chi_\pm$ in our Hamiltonian formalism.

D. Purely edge phase transition

In this section, we provide an interpretation of this gapless edge theory given by Eq. (49) as the critical point between two types of topologically distinct gapped edges of the $\mathbb{Z}_2$ topological order. In the following, we only work with the Wen plaquette model with an open boundary and without any dislocations. The labeling of the edge Majorana modes follows that of Fig. 8. We use the same convention as above that the plaquette on the southeast corner is defined to be even. We consider a generalized edge Hamiltonian

$$H'_{\text{bdy}} = -\sum_{i=1}^{L-1} [1 + (-)^i \lambda] i t_{i,i+1} \xi_i \xi_{i+1} - [1 + (-)^L \lambda] i t_{L,1} \xi_L \xi_1, \quad (68)$$

where λ is a tuning parameter. When $\lambda = 0$, H'_{bdy} reduces back to the Hamiltonian H_{bdy} in Eq. (49) which gives rise to the gapless edge theory. A nonzero λ results in an alternating pattern of the hopping strength in the edge Majorana chain. From now on, we define the links along the edge between the edge Majorana modes ξ_{2r-1} and ξ_{2r} with $r = 1, 2, \ldots, L/2$ as the e links, and the links between the edge Majorana modes ξ_{2r} and ξ_{2r+1} with $r = 1, 2, \ldots, L/2 - 1$, as well as the link between ξ_L and ξ_1, as the m links. In the generalized edge model H'_{bdy}, the hopping strength along the e links is given by $1 - \lambda$, while the hopping strength along the m links is given by $1 + \lambda$. One should always remember that each of the fermion hopping terms can be written in terms of the bosonic operators in Eqs. (47) and (48). Therefore, H'_{bdy} can be expressed using the Pauli matrices on the sites on edge.

For the simplicity of discussion, we can focus on the sector such that the edge Majorana chain has an antiperiodic boundary condition, i.e., $(-)^\Phi = 1$. In this case, we can gauge fix such that $t_{i,i+1} = t_{L,1} = 1$ for all $i = 1, 2, \ldots, L-1$. H'_{bdy} then becomes the standard 1d Majorana chain. When $\lambda \neq 0$, the dispersion of the edge fermions is gapped and, hence, the Hamiltonian H'_{bdy} is gapped as well. It is well known that the phases with $\lambda > 0$ and $\lambda < 0$ are two distinct symmetry-protected-topological (SPT) phases of the 1d Majorana chain. The states with $\lambda > 0$ (or $\lambda < 0$) are all adiabatically connected. The two SPT phases each have a simple limit at $\lambda = 1$ and -1, respectively. With $\lambda = 1$, the hopping along the e links is completely switched off and the edge Majorana modes dimerize on the m links. With $\lambda = -1$, the hopping along the m links is completely switched off and the edge Majorana modes dimerize on the e links instead. One can easily see that the two SPT phases can be mapped into each other by exchanging the roles of the e links and the m links. Therefore, if we enforce a symmetry between e links and the m links in the edge model (which consequently requires $\lambda = 0$ in H'_{bdy}), the edge theory has to be at the critical point between the two SPT phases.

The two SPT phases on the edge and the critical point between them can be reinterpreted in connection to the $\mathbb{Z}_2$ topological order in the bulk. For the phase with $\lambda > 0$, we can take the case with $\lambda = 1$ as a representative. When $\lambda = 1$, the only terms left in H'_{bdy} are the hopping terms on the m links which are exactly the edge terms [shown in Eq. (47)] that are adjacent to the odd plaquettes of the bulk.[3] Remember that we have associated the m particle to the odd plaquette in the bulk. Only turning on the edge terms adjacent to the odd plaquettes in fact enforces the m-condensing (gapped) edge of the toric topological order. Hence, the gapped edge phase with $\lambda > 0$ should be associated to the m-condensing edge of the $\mathbb{Z}_2$ topological order. Following a similar line of reasoning, we can conclude that the gapped edge phase with $\lambda < 0$ should be associated to the e-condensing edge of the $\mathbb{Z}_2$ topological order. The gapless point at $\lambda = 0$ is in fact the critical point between the two types of gapped edges of the $\mathbb{Z}_2$ topological order. Generically, the edge of $\mathbb{Z}_2$ topological order does not need to be at the critical point. However, if we enforce the e-m duality as a "symmetry" of the whole system, there will be a "symmetry" between the e links and the m links on the edge. It enforces a gapless edge that is the critical point between the two types of gapped edges.

ACKNOWLEDGMENTS

W.-Q.C. is supported by National Key Research and Development Program of China (Grant No. 2016YFA0300300) and NSFC (Grants No. 11674151 and No. 11861161001). C.-M.J. is supported by the Gordon and Betty Moore Foundations

[3] In fact, some m links are associated to the corner terms on the corner of even plaquettes. But, it will not change the following discussion.

EPiQS Initiative through Grant No. GBMF4304. L.K. and H.Z. are supported by the Science, Technology and Innovation Commission of Shenzhen Municipality (Grant No. ZDSYS20170303165926217) and by Guangdong Provincial Key Laboratory (Grant No. 2019B121203002). L.K. is also supported by NSFC under Grant No. 11971219. H.Z. is also supported by NSFC under Grants No. 11871078 and No. 11131008.

[1] X. G. Wen, Choreographed entanglement dances: Topological states of quantum matter, Science **363**, eaal3099 (2019).

[2] S. Morrison and D. Penneys, Monoidal categories enriched over braided monoidal categories, Int. Math. Res. Not. **2017**, 1 (2017).

[3] L. Kong and H. Zheng, Gapless edges of 2d topological orders and enriched monoidal categories, Nucl. Phys. B **927**, 140 (2018).

[4] A. Y. Kitaev and L. Kong, Models for gapped boundaries and domain walls, Commun. Math. Phys. **313**, 351 (2012).

[5] L. Kong, Anyon condensation and tensor categories, Nucl. Phys. B **886**, 436 (2014).

[6] E. Plamadeala, M. Mulligan, and C. Nayak, Short-range entangled bosonic states with chiral edge modes and T-duality of heterotic strings, Phys. Rev. B **88**, 045131 (2013).

[7] L. Kong and H. Zheng, A mathematical theory of gapless edges of 2d topological orders Part I, J. High Energy Phys. 02 (2020) 150.

[8] L. Kong and H. Zheng, A mathematical theory of gapless edges of 2d topological orders Part II, arXiv:1912.01760.

[9] A. Y. Kitaev, Fault-tolerant quantum computation by anyons, Ann. Phys. **303**, 2 (2003).

[10] S. B. Bravyi and A. Y. Kitaev, Quantum codes on a lattice with boundary, arXiv:quant-ph/9811052.

[11] M. Barkeshli, E. Berg, and S. Kivelson, Coherent Transmutation of Electrons into Fractionalized Anyons, Science **346** 722 (2014).

[12] A. Y. Kitaev, Anyons in an exactly solved model and beyond, Ann. Phys. **321**, 2 (2006).

[13] P. Etingof, D. Nikshych, and V. Ostrik, On fusion categories, Ann. Math. **162**, 581 (2005).

[14] Y.-Z. Huang, Riemann surfaces with boundaries and the theory of vertex operator algebras, in *Vertex Operator Algebras in Mathematics and Physics*, edited by S. Berman, Y. Billig, Y.-Z. Huang, and J. Lepowsky, Fields Institute Communications (American Mathematical Society, Providence, RI, 2003), Vol. 39, pp. 109–125.

[15] L. Kong, Conformal field theory and a new geometry, in *Mathematical Foundations of Quantum Field and Perturbative String Theory*, edited by H. Sati and U. Schreiber, Proceedings of Symposia in Pure Mathematics (American Mathematical Society, Providence, RI, 2011), Vol. 83, pp. 199–244.

[16] Y.-Z. Huang, Rigidity and modularity of vertex tensor categories, Commun. Contemp Math. **10**, 871 (2008).

[17] Y.-Z. Huang and J. Lepowsky, Tensor products of modules for a vertex operator algebra and vertex tensor categories, in *Lie Theory and Geometry, in Honor of Bertram Kostant*, edited by R. Brylinski, J.-L. Brylinski, V. Guillemin, and V. Kac (Birkhäuser, Boston, 1994), pp. 349–383.

[18] L. Kong and H. Zheng, Drinfeld center of enriched monoidal categories, Adv. Math. **339**, 749 (2018).

[19] W. Ji and X.-G. Wen, Categorical symmetry and non-invertible anomaly in symmetry-breaking and topological phase transitions, arXiv:1912.13492.

[20] L. Kong, T. Lan, X.-G. Wen, Z.-H. Zhang, and H. Zheng, Algebraic higher symmetry and categorical symmetry: A holographic and entanglement view of symmetry, arXiv:2005.14178.

[21] Y.-Z. Huang and L. Kong, Full field algebras, Commun. Math. Phys. **272**, 345 (2007).

[22] F. A. Bais and J. K. Slingerland, Condensate induced transitions between topologically ordered phases, Phys. Rev. B **79**, 045316 (2009).

[23] A. Kirillov Jr. and V. Ostrik, On q-analog of McKay correspondence and ADE classification of $\widehat{sl}_2$ conformal field theories, Adv. Math. **171**, 183 (2002).

[24] L. Kong and I. Runkel, Cardy algebras and sewing constraints, I, Commun. Math. Phys. **292**, 871 (2009).

[25] M. Müger, From subfactors to categories and topology II The Quantum Double of Tensor Categories and Subfactors, J. Pure Appl. Algebra **180**, 159 (2003).

[26] J. Fröhlich, J. Fuchs, I. Runkel, and C. Schweigert, Correspondences of ribbon categories, Adv. Math. **199**, 192 (2006).

[27] E. Rowell, R. Stong, and Z. Wang, On classification of modular tensor categories, Commun. Math. Phys. **292**, 343 (2009).

[28] V. Ostrik, Module categories, weak Hopf algebras and modular invariants, Transform Groups **8**, 177 (2003).

[29] H. Zheng, Extended TQFT arising from enriched multi-fusion categories, arXiv:1704.05956.

[30] Y.-Z. You and X.-G. Wen, Projective non-Abelian statistics of dislocation defects in a $\mathbb{Z}_N$ rotor model, Phys. Rev. B **86**, 161107(R) (2012).

[31] H. Bombin, Topological Order with a Twist: Ising Anyons from an Abelian Model, Phys. Rev. Lett. **105**, 030403 (2010).

[32] Y.-Z. You, C.-M. Jian, and X.-G. Wen, Synthetic non-Abelian statistics by Abelian anyon condensation, Phys. Rev. B **87**, 045106 (2013).

[33] S. Yang, L. Lehman, D. Poilblanc, K. Van Acoleyen, F. Verstraete, J. I. Cirac, and N. Schuch, Edge Theories in Projected Entangled Pair State models, Phys. Rev. Lett. **112**, 036402 (2014).

[34] P. D. Francesco, P. Mathieu, and D. Sénéchal, *Conformal Field Theory* (Springer, Berlin, 1996).

[35] W. Ji and X.-G. Wen, Non-invertible anomalies and mapping-class-group transformation of anomalous partition functions, Phys. Rev. Res. **1**, 033054 (2019).

[36] D. Aasen, R. S. K. Mong, and P. Fendley, Topological defects on the lattice I: The Ising model, J. Phys. A: Math. Theor. **49**, 354001 (2016).